A Unified Model of Cohort Mortality

April 4, 2022

Abstract

We propose a dynamic production function of population health and mortality from birth onwards. Our parsimonious model provides an excellent fit for the mortality and survival curves for both primate and human populations since 1816. The model sheds light on the dynamics behind many phenomena documented in the literature, including (1) the existence and evolution of mortality gradients across socioeconomic statuses, (2) non-monotonic dynamic effects of in-utero shocks, (3) persistent or "scarring" effects of wars and (4) mortality displacement after large temporary shocks such as extreme weather.

JEL: I10, J11

Keywords: Mortality, Health, In-utero shocks, Selection, Scarring.

We propose a coherent framework to understand how population health and mortality evolve from birth onwards, and how economic and other environmental factors throughout life affect this evolution. Statistical and economic models of health and mortality typically only concentrate on adults. Yet a large literature now documents that events and investments in utero and throughout childhood are powerful predictors of both economic and health outcomes later in life (Almond and Currie 2011, Almond et al. 2018). In the absence of such a quantitative model, it is difficult to predict how shocks will affect population health at various ages, and even harder to design optimal investment or compensation policies.

We present a simple dynamic model of the production of health from birth to death for a heterogenous population. In the spirit of classic demographic work (Vaupel et al., 1979), some individuals are born frailer than others. Subsequently, the health distribution of the survivors evolves according to a simple law of motion that depends on the level of external resources, which are stochastic. As in Grossman (1972)'s classic work of the production of health, an individual's health deteriorates with age, but can increase with resources. At any age, individuals in poor health die. In addition, individuals die from reasons unrelated to their health status. During the adolescent years, these "external" causes of death account for a large portion of deaths.

We estimate this model separately for more than 100 birth cohorts born since 1816, using high quality data from the Human Mortality Database. Despite vast changes in life expectancy throughout the period, the model provides an excellent characterization of the age-profiles of mortality for each of these cohorts, and is consistent with the following stylized facts: (1) the profile of log mortality rates by age has a J-shape, and (2) survival curves for humans have "rectangularized" over the last two centuries. They have become flatter throughout life and drop abruptly at older ages.

We then show that simple extensions of the model can generate other previously documented phenomena. Specifically we show that (1) changes in lifetime resources generate

"SES gradients" (persistent gaps in log mortality rates across populations with different socio-economic status) that fall with age; (2) in-utero insults result in non-monotonic impacts on health and mortality over the lifetime; (3) short-term negative shocks (such as wars) that temporarily lower resources result in "scarring" (elevated mortality of survivors); and (4) environmental shocks, such as hot weather, that affect the threshold for dying lead to harvesting (temporarily elevated mortality followed by temporarily lower mortality). The model also describes the evolution of chimpanzee mortality well.

The evolution of mortality over the lifetime is in fact remarkably similar across human populations and across most primates. Because of this regularity, demographers have searched for a "unified" model of mortality (Carnes et al., 1996) that would predict mortality from birth to death at least since the early 19th century. Like much of the following literature (e.g. Li and Anderson, 2013), Gompertz (1825)'s model accounts for mortality *only after a certain age*, focusing on the roughly log-linear portion of the mortality curve after age 40. There are a few exceptions. A popular model by Heligman and Pollard (1980) fits period data mortality rates from various contexts remarkably well. More recent demographic models describe aggregate mortality rates as a function of various parameters albeit with different objectives: Sharrow and Anderson (2016) decompose the gains in longevity into intrinsic and extrinsic deaths, while Palloni and Beltrán-Sánchez (2017) simulate the effects of childhood frailty on mortality throughout life.

Our first contribution to the literature (reviewed in detail in Appendix B) is to provide a new model of cohort mortality. Our approach differs in one fundamental aspect from the demographic approach just described. As in the seminal Grossman (1972) model, we model directly how the health stock of each *individual* evolves, rather than only modeling the mortality or survival rates of the aggregate population. Like Sharrow and Anderson (2016) we decompose mortality into two separate causes of death, extrinsic and intrinsic. Like Palloni and Beltrán-Sánchez (2017) we can use our model to study the effects of frailty. Our model accomplishes both aims within the same framework while achieving a

great fit like Heligman and Pollard (1980)'s model.

The second contribution of this paper is to show that simple modifications of this baseline model account for a wide range of existing demographic phenomena. We demonstrate this by studying the effects of increasing lifetime resources, and the impact of negative in utero shocks on a population's subsequent average health and mortality. We also study the effects of temporary shocks such as wars or bad weather. To our knowledge there is no other model that both provides an excellent fit to the cohort data and that can also explain the variety of phenomena we study.

Our model provides a framework that bridges the demographic and economic approaches: we model individual health as economist do, but we study its aggregate implications for population mortality in the tradition of demographic studies. Our model is more parsimonious than the classic work by Grossman (1972), or its most recent successors in the economics literature (Dalgaard and Strulik, 2014 or Galama and Van Kippersluis, 2019). These more complex models were developed to understand health expenditures and health behaviors. We focus on a production process only and are silent about maximizing behavior, at least initially.

Our main innovation relative to economic models is to include childhood. Alternative state-of-the art models, such as Dalgaard and Strulik (2014)'s accumulating health deficits model, or Galama and Van Kippersluis (2019)'s theory of socioeconomic status and mortality, start with adults. A recent model by Dalgaard et al. (2021) includes childhood, but it does so by adding a separate health production function for childhood. Instead, our framework describes aging from birth to death with a unique law of motion, where mortality declines during childhood due to both selection and investments. We also demonstrate that our model fits mortality curves for entire cohorts well, which economic models have not demonstrated.

This paper proceeds as follows. We start by describing the data and the stylized facts that inform our model. We then describe the model and its properties. Next we show

that the model does an excellent job at matching the mortality profiles of many cohorts. Having established the fit, we describe how the model can be used to understand the effects of permanent (in utero or SES) and temporary (wars and heat waves) changes in the environment. We then briefly describe how a planner would optimally allocate health resources to demonstrate how one could extend our model to include optimization and conclude.

Stylized Facts: Health and Mortality Over the Lifetime

Mortality

We study the evolution of mortality for a given cohort using data from the Human Mortality Database (hereafter HMD). The HMD provides population and death counts by age, birth-year and gender collected through vital registration systems (birth and death certificates) and censuses, from 1816 up to 2015. Despite a few limitations, the HMD is the highest quality data available for cohort analysis. We compute mortality rates by age for each cohort as the number of deaths divided by the population at that age, and use these to compute survival rates and life expectancy (See Appendix D). We focus on French cohorts for two reasons: these cohorts are large and the data goes back to 1816.

We study cohort not period mortality rates, which are used more often. In a stationary environment, with stable mortality rates by age over time, the two are very close, but they diverge otherwise. Appendix Figure 10 summarizes the evolution of period and cohort life expectancy at birth by gender in France.[1] For the 1816-1860 cohorts, (cohort and period) life expectancy at birth was stable around 40 for females and 39 for males. But life expectancy increased in the late 19th century, with cohort life expectancy rising more

[1]Period life expectancy is computed using the cross-sectional mortality rates of all cohorts alive in a given year. Cohort life expectancy is computed using the *realized* mortality rates of a cohort instead. For example, 1850 period life expectancy uses the observed mortality rates of 70 year-olds in 1850. But to compute 1850 cohort life expectancy, the mortality rates at age 70 are those observed in 1920.

than period life expectancy. Several cohorts of men (born roughly 1880-1900) experienced declines in life expectancy, likely due to WWI and WWII. Females born around 1920 lived around 69 years, and males around 59, substantially longer than cohorts born a century earlier.

[Figure 1 about here]

Figure 1 shows the logarithm of mortality rates by age, for selected birth cohorts of women born between 1860 and 1940, for various European countries (panel a) and for France (panel b). Although the level of mortality changed substantially over time, the basic evolution of mortality rates by age is similar across many countries and periods.

For a given cohort, the logarithm of mortality has the shape of a "check mark": high at birth, low among the young, and high and rising almost linearly with age in adulthood. Mortality curves also display an "adolescent hump," especially visible for cohorts born in the 19th century: starting in adolescence, mortality rates jump up (Preston et al. 2000, Thiele, 1871). Finally, there are clearly visible spikes for some cohorts, corresponding to wars and epidemics. These patterns are more visible when examining all the cohort curves, which are similar though not identical for men (see Appendix Figures 11 and 12). These patterns are not unique to humans. Bronikowski et al. (2011) show, using longitudinal data from primates living in the wild, that these patterns of mortality are similar across all primates.

Health

The WHO defines health as "a state of complete physical, mental and social well-being and not merely the absence of disease and infirmity." Thus, health is a multidimensional concept that is not easily captured by any single metric. A striking empirical pattern is that the distribution of various health indicators observed at different ages is roughly Gaussian. For example, the distribution of birth weights is normal (Wilcox and T Russell, 1983) and so is the distribution of adults heights (Tanner and Tanner, 1981).

How does the distribution of health evolve with age? Unfortunately, the HMD does not contain any health measure – there is in fact no data we are aware of that tracks a consistent measure of health from birth to death for a given cohort. But several studies provide partial descriptions of this evolution. Mean health increases and then falls with age, peaking sometime in young adulthood. Biological functions, such as muscle mass (Metter et al., 1999) or bone mass (Baxter-Jones et al., 2011), and performance in physical and cognitive tasks (Strittmatter et al. 2020, Allen and Hopkins 2015), peak sometime between ages 20 and 35. Self-reported measures of health, which capture overall health, decline in adulthood (Deaton and Paxson, 1998, Case and Deaton, 2005, Halliday et al., 2018 and Kaestner et al., 2020).

The variance of health also rises with age, and then seems to level off or fall among the oldest, though the data are less clear about what happens among the oldest (Deaton and Paxson, 1998, Halliday, 2011 and Halliday et al., 2019). The variance in organ function also rises with age (Steves et al. 2012).

Lastly, both objective measures of health and subjective overall measures of health are strong predictors of mortality (Benyamini and Idler, 1999; McGee et al., 1999).

A Unified Model of Aging and Mortality

In this section we present a simple model that can account for these basic "stylized facts" about health and mortality.

A basic model of natural mortality. Individuals are born with an initial health endowment H_0. This initial health endowment differs across individuals in the population and has an unknown distribution.[2]

[2]While health is a multi-dimensional object, we use a single index in the model, as in Grossman (1972). The single-dimension health variable can be viewed as the sufficient statistic for a larger collection of health indicators (vascular, brain functions, lung, etc.), each following in theory a different law of motion. Alternatively one could model various health dimensions and how each affects the probability of dying as in engineering models of aging or competing risks models.

Every period, the environment provides resources I to all individuals, which increase health, H. In this basic model (and in contrast to Grossman's) individuals have no control over their resources. In addition, individuals in the same environment are more or less lucky, and experience an idiosyncratic shock ε_a to their resources. For example I characterizes the per capita amount of food that a country produces, but a given person might receive less if for instance rain was unusually low in their location. The variance of ε_a captures how unequal the distribution of resources is. These idiosyncratic shocks are assumed to be i.i.d. every period.

Finally, the health stock depreciates each period by an amount $d(a)$, which increases with age a ($d'(a) > 0$). This aging process reflects "the accumulation of random damage to the building blocks of life — especially to DNA, certain proteins, carbohydrates and lipids (fats) — that begins early in life and eventually exceeds the body's self-repair capabilities" (Olshansky et al., 2002). Together these forces determine the evolution of the health stock, which is an unobserved latent variable.

Individuals die when their stock of health dips below a threshold $\underline{H}$, which is fixed throughout the lifetime and identical for all individuals. (This assumption that overall health predicts mortality is consistent with empirical observation.) Let $D_a = \mathbb{I}(H_a \leq \underline{H}, D_{a-1} = 0)$ denote the random variable equal to one if the individual dies at age a. Then, the population's health and mortality are characterized by the following dynamic system:

$$\begin{cases} H_a = H_{a-1} - d(a) + I + \varepsilon_a \quad \text{if } D_{a-1} = 0 \\ D_a = \mathbb{I}(H_a < \underline{H}, D_{a-1} = 0), \\ D_0 = 0 \end{cases}$$

with $I \in \mathbb{R}$. Note that if $D_a = 1$ then H_a is undefined – we do not observe the health of individuals after they die. But we observe the mortality rate for the population at age a, which is given by $MR_a = P(D_a = 1 | D_s = 0\,,\, \forall s < a)$. Thus, the distribution of health and

the mortality rate at any age are functions of the entire history of shocks and investments.

We make three key parametric assumptions to make the model more tractable and consistent with the empirical evidence above. First, H_0 follows a normal distribution $\mathcal{N}(\mu_H, \sigma_H^2)$. Second, shocks to resources every period also follow a normal distribution $\varepsilon_a \sim \mathcal{N}(0, \sigma_\varepsilon^2)$.[3] Third, depreciation is a power function $d(t) = \delta a^\alpha$ with $\delta \in (0, \infty), \alpha \in (0, \infty)$.[4] This aging process starts slowly at birth, consistent with evidence that aging markers deteriorate among children (Wong et al., 2010). Then it increases rapidly with age among adults, as in biological models of senescence (Armitage and Doll, 1954; Pompei and Wilson, 2002).[5]

[Figure 2 about here]

Figure 2 illustrates the evolution of health and mortality in the first two periods. Initially, the health distribution is normal. Then it shifts to the right during the first period (as long as I is positive and larger than the aging term) and spreads out (because of the stochastic shock ε_a). Individuals who were born too frail or who experience large negative shocks move to the left of the threshold and die. Graphically, the infant mortality rate (the fraction of individuals who die in the first period) corresponds to the area under the dashed red curve below the threshold. In the second period, this truncated distribution moves right again (if I is large relative to $d(1)$), and the population receives a new shock, generating mortality again among those with large negative shocks.

The stochastic term ε_a therefore plays a key role. In its absence, there would be no deaths in period 2 – nor in any subsequent period, until the depreciation term becomes large enough to push the leftmost part of the distribution below the threshold.[6] Then

[3] Conceptually, the model can accommodate other distributions. But simulations with alternative assumptions (e.g. log normal errors) resulted in counterfactual mortality rates and a poorer overall fit.

[4] Our estimates for human populations find that $\alpha > 1$: the depreciation is therefore convex in age. Many empirical studies in gerontology have focused on the "rate of aging", which in our model corresponds to $\frac{\Delta H}{H} = \frac{-d(a)}{H}$. As in those studies and consistent with Dalgaard et al. (2019) we find that individuals with lower health levels age at a faster rate.

[5] See Gavrilov and Gavrilova (1991) and Weibull (1951) for attempts at biological micro-foundations drawing on reliability theory from engineering.

[6] If I is less than aging, then one could also generate positive mortality in the second period without a stochastic term. But then mortality would be rising from age 2 onwards, which we do not observe in the

mortality increases every period. Eventually everyone dies – this is proved more formally in Appendix .[7]

[Figure 3 about here]

This basic model matches the stylized patterns described above. Figure 3 shows the evolution of the health distribution and the resulting mortality over the lifetime. Just like their empirical counterparts, cohorts in our model exhibit the following patterns: (1) the distribution of health is roughly normal at most ages; (2) mean population health increases and falls with age; (3) the variance of health increases and falls with age; and (4) mortality falls and then rises at a roughly log-linear rate after middle age. There is only one feature of the data that we have not accounted for: the increase in mortality around adolescence, which we consider next.

External causes of death. Not all deaths have direct biological causes. Many deaths, like accidents or homicides, strike individuals regardless of their health status. These "extrinsic" causes of death can be integrated in the model by adding an i.i.d. "accident shock" that is independent of the stock of health H_a. Then a constant fraction $\kappa \in [0, 1]$ of the population is randomly killed every period. This random accident rate places a floor on the level of mortality that is constant across ages.[8] Figure 4a shows that adding a lifetime accident shock increases the level of mortality but does not change its basic evolution. Adding mortality from accidents also does not affect the distribution of health among the living, because these deaths are random and do not depend on health status.

[Figure 4 about here]

Contemporary data however show that the mortality rate from external causes of death is not constant throughout life. Instead, it is well approximated by a step function, with a major increase around adolescence (Figure 4b). Among the young (ages 15-

data.

[7]Because I increases only linearly, but aging increases more than linearly, eventually all individuals die, even lucky ones with many large positive health shocks. This feature is different from the standard Grossman model in which eternal life is possible, as noted by Case and Deaton (2005) or Strulik (2015).

[8]If all health-related deaths were eliminated, this accident rate would uniquely determine the life expectancy of the population ($1/\kappa$).

24), more than 80% of deaths are due to external deaths (Centers for Disease Control and Prevention, 2019). Based on this evidence, we assume that κ starts at zero but becomes positive in adolescence at an arbitrary age (a^*), adding two more parameters to the model. For simplicity, we assume that the onset of adolescence is unaffected by health levels, and we take it to be exogenous.[9] Figure 4a shows that adding this step function results in a profile of mortality that qualitatively matches the main features we observe.[10]

Explaining Mortality Patterns

We now assess whether the model can quantitatively match observed patterns of mortality. We do this by estimating the parameters of the model and assessing the model's fit for both human and primate cohorts. We then compare our model to other models in demography.

Identification and Estimation.

Identification. Two out of the nine parameters of the full model cannot be identified. To see this, note that we can add or subtract any constant, on both sides of the expression that determines the probability of dying $D_a = \mathbb{I}(H_a < \underline{H}, D_{a-1} = 0)$, and leave the mortality rates at all ages unchanged. Thus we must normalize either the level of initial health μ or the threshold $\underline{H}$. Similarly we can multiply each side of the equation by any positive constant and leave the probability of dying unchanged. Therefore the scale of at least one variable must also be normalized. Without loss of generality, we set $\underline{H} = 0$ and $\sigma_H = 1$. After normalization, all the parameters are expressed in "standard deviation" units (except for α and κ, which are "scale free" – they do not depend on the initial distribution).

[9]This assumption could be relaxed. The onset of menarche, a proxy for adolescence in women, has declined from approximately age 16 to age 12 in the last two centuries. This development has been linked to nutritional changes and might be a function of health.

[10]The shapes in the two figures are not identical. However, the contemporary data is not cohort but period data. In contemporary settings, the two profiles differ substantially. But there is no historical cohort mortality data by cause of death to create the more relevant cohort figure.

For example, we interpret μ_H as the distance from the threshold of the initial distribution, in standard deviations of the initial distribution.

The rescaled model characterizes the biological evolution of health and mortality of a cohort using 7 (rescaled) parameters: one for the mean initial health (μ_H), two governing the aging process (δ, α), two characterizing the effects of resources, in the form of average investments (I) and the variance of these investments (σ_ε^2), and finally two capturing the accident rate (κ) that starts in adolescence at age $a*$. We do not estimate this last parameter. For women, we assume adolescence occurs at menarche, which starts at age = (- 0.0175 x calendar year) + 47.4. This equation was estimated by de La Rochebrochard (2000) using historical data from multiple sources. Adolescence is assumed to start one year later for men, as observed in contemporary settings. For chimpanzees we use two alternative start dates, age 8 and age 14, which span the ranges described in the literature.[11]

Estimation. Despite the model's conceptual simplicity, the mortality rate at a given age cannot be expressed in closed-form.[12] We therefore estimate the parameters using the simulated method of moments: we generate data for a population and compare the resulting survival curve to the actual survival curve. The program iterates over the parameter space until the difference between the simulated data and the actual data is minimized. By matching the age-specific survival rates we implicitly match life expectancy. See Appendix D for details.

Mortality Rates Over the Lifetime

We start by estimating the model for women born in 1816. The model closely matches their mortality rates at every age (Figure 5a). The predicted life expectancy is 38 years and 102 days compared to the actual life expectancy of 38 years and 91 days.

[11] Bronikowski et al. (2011) report the onset at age 14. Other sources (Behringer et al., 2014) place the onset at age 8.

[12] Our model is similar to a class of models used for corporate default probability and securities pricing. This literature has established that, except for the particular case of a constant or linear drift, these models do not admit closed-form solutions (see Lando, 2004).

We estimate an initial mean health of 0.86, so many individuals are born at or below the threshold (Appendix Table 1). Absent any shocks or investment in the first period, infant mortality would have been roughly 15% (instead of 17%). Mortality falls dramatically after age 1 because there is selection (many frail individuals have already died), and because investment is large relative to aging in the first period (I is estimated as 0.4 and δ as 0.0006).[13] The estimated variance of resources is large (~1) so a few unlucky individuals still fall below the death threshold after age 2. Log mortality starts a steady increase after age 45. This occurs because while δ is small (~ 0.0006) the aging rate α is around 1.8, so that the aging function δt^{α} is increasing more than linearly with age.

Accounting for external deaths is important – the fit of the model improves significantly and the estimated parameters change when we do (comparing column 1 and 2 of Appendix Table 1). The external mortality rate is 8.6 per thousand per year, lowering this cohort's life expectancy by about 7.6 years. This provides an upper bound estimate of the effect of maternal mortality – the main cause of death for women in the 19th century – on life expectancy in the past.

These results are robust to a number of alternative estimation modifications including using alternative weights, using an alternative objective function, and allowing for truncation at age 90. We also estimate models where the onset of adolescence is normally distributed and estimated. These results (in Appendix Table 2) show that the fit is not very sensitive to these alternatives.

Gender differences. Appendix Figures 13a show the results for males born in 1816 (Appendix Table 1 reports the estimated parameters). Men born in 1816 lived shorter lives than women (Goldin and Lleras-Muney 2019, Cullen et al. 2016). After accounting for the adolescent hump (column 4), we find that males' initial mean health is 18% lower than that of females', consistent with their greater frailty and higher infant mortality rates. Males receive slightly larger annual investments (about 10% greater) but ex-

[13] Note that health investments I are not technically needed to generate declining mortality in childhood.

perience greater variance in investments (5%). They also age faster in old age (though women age a bit faster during prime ages). The increase in deaths in adolescence is larger for men ($\kappa = 0.0097$), consistent with their greater involvement in accidents and violent deaths.[14] However, because males have higher overall mortality rates, the elimination of accidental deaths would increase their life expectancy by about 7.6 years, similar to the predicted gains for women.

Overall, the model fit is excellent for both genders, though the fit is better for females. It shows that almost all parameters benefit women's survival except for mean investments.

[Figure 5 about here]

Primates. Our model should describe primate mortality well: they live in relatively stable environments, experience no technological change and have few optimization opportunities. Primate mortality patterns are also similar to humans'. We use the best available data on chimpanzees living in the wild from Bronikowski et al. (2011) to estimate the model. These populations are tracked in the wild from birth to death and have been used to compare mortality across various primate populations. We focus on chimpanzees because they are the closest primates to humans.

We obtain a very good fit, despite the smaller population size and therefore much noisier estimates (see Appendix Figure 13b and Appendix Table 3). Compared to human females, female chimps are born in better health, consistent with the observation that human infants are born frail relative to other species.[15] They have a lower rate of accidental deaths, in line with the fact that maternal mortality is a uniquely important problem among humans (Rosenberg, 1992).[16] But other parameters favor longevity among human females. In chimps, the estimated annual investment (I) is ~20% smaller and the variance

[14] Accounting for the adolescent hump significantly improves the fit, as was the case for women (column 4 v. 3).

[15] There are several theories for this – for a discussion, see Rosenberg and Trevathan (1995).

[16] As Rosenberg (1992) puts it, "most primates experience parturition as a simpler, shorter, and very likely less painful process (than humans)." Our estimates do not imply that external causes of death are unimportant among primates—neither model estimates a baseline accident rate throughout.

of I is 10% larger than among humans. Most notably, δ is much larger (0.06 v. 0.0006) than in humans, resulting in much faster aging.

As in humans, female chimps live longer than males, partly because males have larger external causes of death than females.[17] Males also have larger annual investments, larger variance in resources and larger aging (α) than females. But unlike humans, males have larger initial health.

The Rectangularization of Survival and the Sources of Increases in Life Expectancy

Remarkably, the model is able to track the evolution of the mortality profiles for all the cohorts born since 1816. This evolution is characterized by a "rectangularization" of the survival curves. Figure 5b illustrates this using the survival curves of French women born in 1816, 1860, 1900 and 1940. Survival to age 1 has increased dramatically. The next section of the survival curve – roughly from age 1 to age 60 – has flattened considerably. In addition, a steep downward slope emerged among the oldest. As a result, more than 70% of those born in 1940 live past age 70, whereas in the 1816 cohort fewer than 30% did. The model captures this rectangularization accurately: the observed (blue markers) and estimated (red dashes) survival curves are very similar for all cohorts. The results are similar for men (Appendix Table 4).[18]

[Figure 6 about here]

What are the sources of increases in longevity according to our estimates? Health at birth μ_H was stagnant for most of the 19th century and then increased dramatically around 1900 (Figure 5c). But μ_H dropped for cohorts born during epidemics (1858, 1870, 1918), extreme weather events (like the extremely hot summer of 1911) and wars (1870, WWI and WWII). These patterns mirror the evolution of infant mortality. It fell after 1900,

[17] Not surprisingly, correctly timing the onset of adolescence is not important for females, but makes a substantial difference for males.

[18] A full examination of gender differences in the estimated time series is beyond the scope of this paper.

as a result of improvements in water, sanitation, and the dissemination of best infant feeding practices (breastfeeding, milk pasteurization, water boiling) which reduced infectious disease mortality (Preston and Van de Walle, 1978, Viazzo et al., 1993, Kesztenbaum and Rosenthal, 2017). And it increased during wars, pandemics and hot summers.

We also observe a secular decline in external causes of death (Figure 5d), consistent with the elimination of maternal mortality (a major cause of death among prime-age women in the past (Loudon, 1988), and with the decline in violent deaths documented by Pinker (2011). This decline tracks the decline in the probability of dying among 15 to 24 year-olds (solid line). The level of κ is similar to the level of mortality among the young, as predicted by the model and in line with contemporary data (Figure 4a).

Lastly we observe a substantial decrease in the force of aging before 1840 and after 1900, the causes of which are unclear (we plot it at age 60: $\delta(60)^{\alpha}$ in panel e). Since food consumption and heights were rising, this suggests that nutrition is a possible determinant of the aging function (Fogel, 1994). Interestingly the aging function declines around 1900 at the same time μ_H rises and infant mortality declines, consistent with Finch and Crimmins (2004) who show "strong associations between early-age mortality and subsequent mortality in the same cohorts" due to the decline in exposure to infectious diseases, which lead to inflammation.

By contrast, health resources (I) did not change much in the 19th century (they fall a bit and rise again), consistent with the debate on the questionable benefits of the Industrial Revolution on health and living standards. However events like the WWI/1918 flu pandemic decrease these resources substantially while they are taking place. Figure 5f shows that there is a substantial temporary decline in I at this time, which is greatest among individuals ages 20 to 40 consistent with the observation that the 1918 pandemic had its largest effects among prime age adults (Murray et al., 2006).

Finally, there is a steady decline in the variance of health resources – it is also unclear why this occurred, though it is possible food availability became less variable (Appendix

Figure 14).[19] These last two parameters (I, σ) are hardest to assess against external data because they represent the distribution of health resources over a lifetime.[20]

Appendix Figure 15 shows the performance of the model for cohorts born 1816-1923 (the last cohort with complete data up to age 90). The fit is excellent throughout the 19th century, but deteriorates after 1900 for a few reasons. First, two events in the early 20th century are likely to severely affect these cohorts: WWI/1918 flu pandemic, and WWII. We discuss below how we estimated these, but these events are difficult to model. The data during these episodes is also of lower quality, as changes in territory, for example, make the computations of death rates difficult. Lastly, we assume that there is no inter-temporal optimization taking place. The rise of social insurance programs throughout the 20th century suggests that this assumption is likely violated for recent cohorts. We discuss optimization and its effects at the end of the paper.

Comparison with alternative demographic models.

We compare the fit of our model to the classic Gompertz (1825) model, the popular Heligman and Pollard (1980) model (HP), a subsequent model developed by Carriere (1992) and the vitality model by Sharrow and Anderson (2016) (SA) (See Appendix B). We estimate these 4 models and ours for men and women born in 1816 and 1921. We compute 3 measures of fit: the RMSE of the survival curve, the RMSE of the log mortality rates and the predicted life expectancy.

The results (in Appendix Table 6) show that the HP model provides the best fit for all cohorts, but our model is very close, and performs better than more recent models. However, unlike the HP model, we can achieve other aims of recent demographic mod-

[19] Alternatively it might be difficult for the model to separately identify the effects of I from the effects of its variance, because the data on mortality is only informative about the left tail of the health distribution.

[20] Their estimation could be improved upon by imposing that overlapping cohorts share the same resources. However, this is not a trivial exercise that requires making additional assumptions and altering the estimation procedure to simultaneously estimate several hundreds of parameters. We leave this to future research.

els. We separate causes of death into two broad categories like SA. In the next section we demonstrate the model's ability to predict frailty effects (which Palloni and Beltrán-Sánchez (2017) study) and to account for other demographic patterns.

Understanding Mortality Dynamics

In this section, we conduct a series of qualitative exercises to demonstrate that the model can rationalize the effects on mortality of temporary and permanent shocks documented in the literature, as resulting from simple shocks to the model parameters.

Socio-Economic Status Mortality Gradient

A substantial literature documents health and mortality "gradients" – large and persistent differences across individuals with different levels of socio-economic status, such as education or income (Cutler et al., 2012).

How can the model rationalize such gradients? Suppose that we extend our model so that higher income leads to higher I throughout life. In other words, assume there exists a function $I = I(Y, E)$ with $I' > 0$ for all inputs such as income Y or education E. We illustrate the effect of lowering Y by simulating the effect of lowering I by 50% for the 1816 French female cohort (Figure 6). This results in higher and flatter log-mortality curves for the poorer population (panel a). Moreover, the curves for the rich and the poor converge in old age, as documented by Chetty et al. (2016) (panel b). This occurs because, although the frailest individuals are killed in the first period when Y falls (potentially lowering mortality), Y shifts the distribution of health left in all subsequent periods, increasing mortality thereafter.

When looking at the profile over the lifetime (Figure 6c), the narrowing of the mortality gap occurs in the model *only after a certain age*. In logs (percentage) terms, the mortality gap initially grows with age but eventually falls. In *levels* however, SES gaps in mortality

rates are U-shaped (instead of hump-shaped) with age, as illustrated by Kaestner et al. (2020) (for education) and hypothesized by the cumulative advantage hypothesis (Lynch 2003, Ross and Wu 1995). The reason the patterns differ in levels and logs is that the log specification captures percentage changes, dividing the SES gaps in levels by the baseline mortality, which is also U-shaped.

[Figure 7 about here]

Health. Lower income (or education) and thus lower I also lowers average health at all ages. But the effect increases with age, and then declines in both levels and percentage terms because mortality starts rising (Figure 6d). These predictions match the evidence in Case et al. (2002), Currie and Stabile (2003) and House et al. (2005), who show that health gaps between those born in poor families and those born in rich families grow with age, but decline after 65.

Resource scarcity or accelerated aging? Higher SES is associated with more frequent physical exercise, lower exposure to pollution and lower stress, which may affect the rate of depreciation (instead of the level of resources).[21] In the model, an increase in the aging parameters (δ or α) and a decrease in I generate similar changes in the health and mortality profiles among the old, as shown Appendix Figure 16. But higher aging rates do not result in any visible health or mortality gaps among children, whereas higher I does. Therefore, the evidence in Case et al. (2002) or Currie and Stabile (2003), interpreted through the lens of the model, suggests that changing family income is equivalent to changing I, though both processes could be at play.

Before moving on, we note that it would be ideal to re-estimate our model using cohort data by education or income — however, there is no data tracking *cohorts* from birth to death by family income or education levels.[22] Our simulations only show that the model

[21] For example Liu et al. 2019 find that education and race are associated with lower methylation rates, a biomarker for aging.

[22] There are a few longitudinal data sets tracking individuals from birth onwards, but they do not provide annual data.

can rationalize the observed patterns in the data.[23]

Changes in I at older ages. We can also easily use the model to study the effects of permanent changes in resources that occur at a specific age. For example, Schwandt and Von Wachter (2020) estimate the effects of entering the labor market during the 1983 recession on lifetime mortality. They use our model to show that a 1% reduction in I at age 18 generates the same effects.

Non-Monotonic Effects of In-Utero Shocks

[Figure 8 about here]

Detrimental events in-utero (famines, war, recession, etc.) result in large and persistent declines in health that are visible in infancy and old age (Barker et al., 1993) and in elevated mortality among the survivors. Empirically these effects are initially large and then appear to "fade out", only to re-appear later in life. (See Almond et al. (2018)'s comprehensive review.) But as Almond and Currie (2011) point out, the Grossman model predicts immediate declines in health that become hardly visible in adulthood (Figure 7a).

What does our model predict? Suppose that we allow for the initial mean of the distribution, μ_H, to be affected by outside forces F ($\mu_H = \mu(F)$ with $F' > 0$). We use the 1816 parameters to simulate the effect of exogenously lowering F and thus μ_H, on the subsequent health and mortality of the survivors (Figure 7b). Lowering initial health μ_H by 50% lowers health among the survivors at all ages — both in levels and in percentages — with a u-shaped pattern in age, exactly as the literature documents. For example Schiman et al. (2017), who study the effects of experiencing WWII in utero and early childhood, find that its effects on health, disability, and employment are not visible for young adults, but grow with age, as predicted here. The reason this happens in our model — but not in

[23] One could also re-estimate the model for the aggregate data as a mixture of the evolution of two populations with different SES levels. However in the absence of data by SES, this would only add more parameters to the model.

Grossman's — is that depreciation in our model is not multiplicative in the stock. Like ours, Dalgaard et al. (2019)'s model of health deficits also predicts that in-utero shocks will result in health gaps that increase with age among adults. But our model predicts a U-shape pattern of effects rather than a monotonically increasing effect. This U-shape results from our having an early childhood period where investments move the distribution of health up.[24] These results also suggest it is not possible to identify the effects of in-utero shocks with health data for adolescents or young adults only.

Mortality. Mortality at all ages also increases when initial conditions worsen (Figure 7c). Again, the age-patterns depend on the metrics used. When measured in levels, the effects are U-shaped. The intuition for this is simple. Among adolescents and young adults, the average level of health is high and very few individuals are close to the threshold, so shifting the distribution of health has very little impact on mortality. But shifts in the distribution will result in higher death rates as the distribution gets closer to the threshold at older ages. When expressed in percentage terms however, the predicted effects of negative in-utero shocks on mortality fall with age, though this pattern is not necessarily monotonic: in middle ages, when mortality levels are low, the effects can rise and fall due to small samples.

An important implication of our simulations for the empirical literature is that the predictions for the dynamic effects of shocks on mortality are sensitive to the functional form one chooses to study its effects.

Scarring Effects of Wars

Wars have long-lasting detrimental health effects among survivors. Such "scarring" effects have been documented in at least 13 European countries after WWII. Compared to less exposed survivors, individuals who were more exposed to the war experienced worse economic and health outcomes that persisted several decades later (e.g. Kesternich

[24] With data on overall health over the lifetime, these different predictions could be verified.

et al., 2014, Havari and Peracchi, 2017). Similarly Wilson et al. (2014) show the persistence of higher mortality rates of WWI on New Zealand for military personnel who served during the war, compared with those that did not.[25]

Suppose we model war episodes as reducing health resources (I).[26] Figure 8a shows the mortality curves obtained from estimating the model for men born in 1896 with two shocks: a 4-year decline in I at age 18 (corresponding to the combined effects of WWI and the 1918 flu pandemic) and a 6-year decline in I at age 43 (corresponding to WWII). This simple characterization of the wars delivers a mortality curve (red dotted line) that is remarkably close to the data (blue line). When the war shocks are shut down, mortality falls during the war and at all subsequent ages (red dashed line). Thus, the model predicts the scarring effects that previous authors have documented: the mortality rates for the affected cohort are persistently higher than those of unaffected cohorts, both during the war and after. We estimate that WWI lowered life expectancy by approximately 16 years for this cohort, and WWII lowered it by another 2 years.[27]

Harvesting Effects

Extreme weather or pollution events appear to displace the distribution of deaths in the short term, creating a sudden increase in the number of deaths followed by abnormally low mortality. In demography, this phenomenon is known as "harvesting" and has been, for instance, documented in France during the 2003 heatwave, as shown in Appendix Figure 17a, reproduced from Toulemon and Barbieri (2008).[28]

How can the model rationalize this pattern? Suppose that the death threshold $\underline{H}$ is a

[25] Costa (2012) also documents scarring effects of the American Civil War on surviving soldiers.

[26] This assumption is consistent with historical data for WWII. GDP declined substantially during the war and 20% to 55% of it was appropriated by Germans during the occupation (Occhino et al., 2007). Food rationing began in 1940. We can assume that the war is a different type of shock, but we do not obtain substantially better fit with these alternatives.

[27] The fit for this cohort can be improved if we allow every year of a war to have its own effect instead of imposing an equal annual shock during wars (Appendix Table 5).

[28] See Schwartz (2000) or Zeger et al. (1999) for the effects of pollution, and Deschênes and Moretti (2009) or Deschênes and Greenstone (2011) for the effects of very hot or very cold weather.

function of the environment ($\underline{H}$=$\underline{H}(E)$, $\underline{H}' > 0$). Appendix Figure 17b shows the simulated effect of a temporary increase in the threshold at ages 60 and 61 on the mortality of the 1816 cohort. It results in very high mortality initially. But mortality starts dropping before the shock ends because the frailest individuals have already died. Once the weather disruption ends, and the threshold is restored to its original (lower) level, mortality falls even more because there are very few individuals close to the new lower threshold. This holds true until the aging process lowers health stocks again. Thus a change in the death threshold generates harvesting, and does so by killing the least healthy individuals of the cohort. A key characteristic of a threshold change is that it does not affect the health of the living.[29]

Heat waves and other forms of bad weather also generate excess mortality among children (Appendix Figure 17c). However, the displacement effect is substantially more spread out among children. In other words, the children who die as a result of the bad weather would not be dying immediately right after the bad weather ends — they would be living substantially longer lives (among children, investment levels are high relative to depreciation and mortality is falling, whereas depreciation is large among the elderly and their mortality is increasing).

The Effects of Temporary and Permanent Shocks

The previous two sections illustrate the effects of temporary changes in I or $\underline{H}$, but do not compare their effects in the same scale because we aimed to reproduce published results. Appendix Figure 18 shows how log mortality rates respond to all types of temporary shocks. Each shock leaves a unique imprint on mortality rates. Temporary investment and depreciation decreases have similar scarring effects: mortality rises when the shock starts and then starts falling after the shock ends, but it does not return to its counterfac-

[29] Weather shocks may affect the health of those who do not die. See Deschênes and Moretti (2009) or Deschênes and Greenstone (2011) for a discussion.

tual level. On the other hand, only changes in the threshold generate harvesting. Only variance changes result in a "cross over" in mortality rates in old ages. And only accident increases leave mortality rates unchanged once the shock ends. Appendix Figure 19 further reveals that the pattern of these responses over time is not the same when viewed in logs or in levels. For comparison Appendix Figure 20 shows the effects of permanent shocks to all parameters, in levels and in logs.

Optimization

So far we considered a population that receives constant investments/resources in its health, uniformly over the lifetime. In Appendix E we estimate the optimal investment profile that a social planner would choose in order to maximize life expectancy. We assume the planner has a fixed lifetime budget and the ability to borrow and save costlessly,[30] and can choose to invest different levels of I at different ages so long as they add up to the total budget. We find that to maximize life expectancy, it is optimal to redistribute resources from prime age adults to children and to the elderly. Doing so would increase the life expectancy for French women born in 1816 by three years – a considerable but smaller gain than is observed in the data. After optimization the resulting survival curves are flatter in adulthood and steeper in old ages, suggesting the rectangularization of survival is partly due to the emergence of optimization.

Conclusion

This paper proposes a parsimonious production function to study the evolution of health and mortality over the life course of a population born with heterogeneous health endowments. Despite its simplicity, this model tracks the evolution of the mortality profile of human cohorts born 1816 to 1940, as well as other species, and it can explain many im-

[30] This is a standard assumption, e.g. see Murphy and Topel (2006).

portant mortality patterns documented in the literature, including the rectangularization of survival curves and SES gradients in health. We also show how to use the model to understand the dynamic treatment effects of in-utero shocks and other temporary events like wars.

The parsimony of the model relies on transparent but strong parametric assumptions. In particular, we assumed that the environment is stable and exogenously provides a constant level of resources. This is reasonable for primates or early human populations, but not for contemporary populations with access to saving technologies, growing GDP and medical innovations. We explored how to incorporate changes in the environment into the model, but further progress could be made by using data on environmental changes as inputs and by making restrictions across cohorts. We also assume that health shocks are i.i.d and normally distributed. Alternative assumptions for this distribution of annual shocks could be further investigated. The model can be also expanded to consider the role of behavior and policy. Our preliminary analysis suggests that, in the absence of financial frictions, optimal health expenditures are U-shaped over the lifetime in this model. With additional data, the implications of optimizing behavior could be explored further. We leave these to future research.

References

Alemayehu, Berhanu and Kenneth E. Warner, "The lifetime distribution of health care costs," *Health services research*, 2004, *39* (3), 627–642.

Allen, Sian V and Will G Hopkins, "Age of peak competitive performance of elite athletes: a systematic review," *Sports Medicine*, 2015, *45* (10), 1431–1441.

Almond, Douglas and Janet Currie, "Killing me softly: The fetal origins hypothesis," *The Journal of Economic Perspectives*, 2011, *25* (3), 153–172.

_ , _ , and Valentina Duque, "Childhood circumstances and adult outcomes: Act II," *Journal of Economic Literature*, 2018, *56* (4), 1360–1446.

Armitage, Peter and Richard Doll, "The age distribution of cancer and a multi-stage theory of carcinogenesis," *British journal of cancer*, 1954, *8* (1), 1.

Barker, David JP, Keith M Godfrey, Peter D Gluckman, Jane E Harding, Julie A Owens, and Jeffrey S Robinson, "Fetal nutrition and cardiovascular disease in adult life," *The Lancet*, 1993, *341* (8850), 938–941.

Baxter-Jones, Adam DG, Robert A Faulkner, Mark R Forwood, Robert L Mirwald, and Donald A Bailey, "Bone mineral accrual from 8 to 30 years of age: an estimation of peak bone mass," *Journal of Bone and Mineral Research*, 2011, *26* (8), 1729–1739.

Behringer, Verena, Tobias Deschner, Caroline Deimel, Jereon MG Stevens, and Gottfried Hohmann, "Age-related changes in urinary testosterone levels suggest differences in puberty onset and divergent life history strategies in bonobos and chimpanzees," *Hormones and behavior*, 2014, *66* (3), 525–533.

Beltrán-Sánchez, Hiram, Eileen M Crimmins, and Caleb E Finch, "Early cohort mortality predicts the rate of aging in the cohort: A historical analysis," *Journal of developmental origins of health and disease*, 2012, *3* (5), 380–386.

Benyamini, Yael and Ellen L Idler, "Community studies reporting association between self-rated health and mortality: additional studies, 1995 to 1998," *Research on aging*, 1999, *21* (3), 392–401.

Bronikowski, Anne M., Jeanne Altmann, Diane K. Brockman, Marina Cords, Linda M. Fedigan, Anne Pusey, Tara Stoinski, William F. Morris, Karen B. Strier, and Susan C. Alberts, "Aging in the natural world: comparative data reveal similar mortality patterns across primates," *Science*, 2011, *331* (6022), 1325–1328.

Carnes, Bruce A., S. Jay Olshansky, and Douglas Grahn, "Continuing the search for a law of mortality," *Population and Development review*, 1996, pp. 231–264.

Carriere, Jacques F., "Parametric models for life tables," *Transactions of the Society of Actuaries*, 1992, *44*, 77–99.

Case, Anne and Angus S Deaton, "Broken down by work and sex: How our health declines," in "Analyses in the Economics of Aging," University of Chicago Press, 2005, pp. 185–212.

_ **, Darren Lubotsky, and Christina Paxson**, "Economic status and health in childhood: The origins of the gradient," *The American Economic Review*, 2002, *92* (5), 1308–1334.

Centers for Disease Control and Prevention, "Percentage of Deaths from External Causes, by Age Group ? United States, 2017," *MMWR Morb Mortal Wkly Rep*, 2019.

Chetty, Raj, Michael Stepner, Sarah Abraham, Shelby Lin, Benjamin Scuderi, Nicholas Turner, Augustin Bergeron, and David Cutler, "The association between income and life expectancy in the United States, 2001-2014," *Jama*, 2016, *315* (16), 1750–1766.

Costa, Dora L, "Scarring and mortality selection among Civil War POWs: A long-term mortality, morbidity, and socioeconomic follow-up," *Demography*, 2012, *49* (4), 1185–1206.

Cullen, Mark R, Michael Baiocchi, Karen Eggleston, Pooja Loftus, and Victor Fuchs, "The weaker sex? Vulnerable men and women's resilience to socio-economic disadvantage," *SSM-population health*, 2016, *2*, 512–524.

Currie, Janet and Mark Stabile, "Socioeconomic Status and Child Health: Why Is the Relationship Stronger for Older Children?," *The American Economic Review*, 2003, *93* (5), 1813–1823.

Cutler, David M., Adriana Lleras-Muney, Tom Vogl, S. Glied, and P. C. Smith, "Socioeconomic Status and Health: Dimensions and Mechanisms.," in "The Oxford Handbook of Health Economics," Oxford University Press, 2012.

Dalgaard, Carl-Johan and Holger Strulik, "Optimal aging and death: understanding the Preston curve," *Journal of the European Economic Association*, 2014, *12* (3), 672–701.

_ **, Casper Worm Hansen, and Holger Strulik**, "Accounting for fetal origins: Health capital vs. health deficits," *Health Deficits (October 19, 2019)*, 2019.

_ **,** _ **, and** _ , "Fetal origins?A life cycle model of health and aging from conception to death," *Health Economics*, 2021, *30* (6), 1276–1290.

de La Rochebrochard, Elise, "Age at puberty of girls and boys in France: Measurements from a survey on adolescent sexuality," *Population: An English Selection*, 2000, pp. 51–79.

Deaton, Angus S. and Christina H. Paxson, "Aging and inequality in income and health," *The American Economic Review*, 1998, *88* (2), 248–253.

Deschênes, Olivier and Enrico Moretti, "Extreme weather events, mortality, and migration," *The Review of Economics and Statistics*, 2009, *91* (4), 659–681.

_ **and Michael Greenstone**, "Climate change, mortality, and adaptation: Evidence from annual fluctuations in weather in the US," *American Economic Journal: Applied Economics*, 2011, *3* (4), 152–85.

Dobkin, Carlos, Amy Finkelstein, Raymond Kluender, and Matthew J Notowidigdo, "The economic consequences of hospital admissions," *American Economic Review*, 2018, *108* (2), 308–52.

Field, Erica, Omar Robles, and Maximo Torero, "Iodine deficiency and schooling attainment in Tanzania," *American Economic Journal: Applied Economics*, 2009, *1* (4), 140–169.

Finch, Caleb E. and Eileen M. Crimmins, "Inflammatory exposure and historical changes in human life-spans," *Science*, 2004, *305* (5691), 1736–1739.

Finch, Caleb E, Malcolm C Pike, and Matthew Witten, "Slow mortality rate accelerations during aging in some animals approximate that of humans," *Science*, 1990, *249* (4971), 902–905.

Fogel, Robert W., "Economic Growth, Population Theory, and Physiology: The Bearing of Long-Term Processes on the Making of Economic Policy," *The American Economic Review*, 1994, *84* (3), 369–395.

Galama, Titus J and Hans Van Kippersluis, "A theory of socio-economic disparities in health over the life cycle," *The Economic Journal*, 2019, *129* (617), 338–374.

Gavrilov, Leonid A and Natalia S Gavrilova, "The reliability theory of aging and longevity," *Journal of theoretical Biology*, 2001, *213* (4), 527–545.

Gavrilov, Leonid Anatolevich and Natalia Sergeevna Gavrilova, *The biology of life span: a quantitative approach.*, Harwood Academic Publisher New York, 1991.

Goldin, Claudia and Adriana Lleras-Muney, "XX> XY?: The changing female advantage in life expectancy," *Journal of health economics*, 2019, *67*, 102224.

Gompertz, Benjamin, "On the nature of the function expressive of the law of human mortality, and on a new mode of determining the value of life contingencies," *Philosophical transactions of the Royal Society of London*, 1825, *115*, 513–583.

_ , "On one uniform law of mortality from birth to extreme old age, and on the law of sickness," *Journal of the Institute of Actuaries and Assurance Magazine*, 1871, *16* (5), 329–344.

Grossman, Michael, "On the concept of health capital and the demand for health," *Journal of Political economy*, 1972, *80* (2), 223–255.

_ , "The demand for health, 30 years later: a very personal retrospective and prospective reflection," *Journal of health economics*, 2004, *23* (4), 629–636.

Halliday, Mark H, Alessandra N Garcia, Anita B Amorim, Gustavo C Machado, Jill A Hayden, Evangelos Pappas, Paulo H Ferreira, and Mark J Hancock, "Treatment effect sizes of mechanical diagnosis and therapy for pain and disability in patients with low back pain: a systematic review," *journal of orthopaedic & sports physical therapy*, 2019, *49* (4), 219–229.

Halliday, Timothy, "Health inequality over the life-cycle," *The BE Journal of Economic Analysis & Policy*, 2011, *11* (3).

_ **, Bhashkar Mazumder, and Ashley Wong**, "Intergenerational health mobility in the US," 2018.

Hartwig, Jochen and Jan-Egbert Sturm, "Testing the Grossman model of medical spending determinants with macroeconomic panel data," *The European Journal of Health Economics*, 2018, *19* (8), 1067–1086.

Havari, Enkelejda and Franco Peracchi, "Growing up in wartime: Evidence from the era of two world wars," *Economics & Human Biology*, 2017, *25*, 9–32.

Heligman, Larry and John H. Pollard, "The age pattern of mortality," *Journal of the Institute of Actuaries*, 1980, *107* (01), 49–80.

House, James S, Paula M Lantz, and Pamela Herd, "Continuity and change in the social stratification of aging and health over the life course: evidence from a nationally representative longitudinal study from 1986 to 2001/2002 (Americans' Changing Lives Study)," *The Journals of Gerontology Series B: Psychological Sciences and Social Sciences*, 2005, *60* (Special_Issue_2), S15–S26.

Human Mortality Database. University of California, Berkeley (USA), and Max Planck Institute for Demographic Research (Germany). Available at www.mortality.org. Data downloaded in August 2017.

Kaestner, Robert, Cuiping Schiman, and Jason Ward, "Education and health over the life cycle," *Economics of Education Review*, 2020, *76*, 101982.

Kesternich, Iris, Bettina Siflinger, James P Smith, and Joachim K Winter, "The effects of World War II on economic and health outcomes across Europe," *Review of Economics and Statistics*, 2014, *96* (1), 103–118.

Kesztenbaum, Lionel and Jean-Laurent Rosenthal, "Sewers? diffusion and the decline of mortality: The case of Paris, 1880–1914," *Journal of Urban Economics*, 2017, *98*, 174–186.

Lando, David, *Credit Risk Modeling: Theory and Applications*, Princeton University Press, 2004.

Li, Ting and James Anderson, "Shaping human mortality patterns through intrinsic and extrinsic vitality processes," *Demographic research*, 2013, *28*, 341–372.

Liu, Zuyun, Brian H Chen, Themistocles L Assimes, Luigi Ferrucci, Steve Horvath, and Morgan E Levine, "The Role of Epigenetic Aging in Education and Racial/Ethnic Mortality Disparities Among Older US Women," *Psychoneuroendocrinology*, 2019.

Loudon, Irvine, "Maternal mortality: 1880–1950. Some regional and international comparisons," *Social history of medicine*, 1988, *1* (2), 183–228.

Lynch, Scott M, "Cohort and life-course patterns in the relationship between education and health: A hierarchical approach," *Demography*, 2003, *40* (2), 309–331.

Makeham, William Matthew, "On the law of mortality and the construction of annuity tables," *Journal of the Institute of Actuaries*, 1860, *8* (6), 301–310.

_ , "On the law of mortality," *Journal of the Institute of Actuaries*, 1867, *13* (6), 325–358.

McGee, Daniel L, Youlian Liao, Guichan Cao, and Richard S Cooper, "Self-reported health status and mortality in a multiethnic US cohort," *American journal of epidemiology*, 1999, *149* (1), 41–46.

Metter, E Jeffrey, Nicole Lynch, Robin Conwit, Rosemary Lindle, Jordan Tobin, and Ben Hurley, "Muscle quality and age: cross-sectional and longitudinal comparisons," *Journals of Gerontology Series A: Biomedical Sciences and Medical Sciences*, 1999, *54* (5), B207–B218.

Mitnitski, Arnold, Joanna Collerton, Carmen Martin-Ruiz, Carol Jagger, Thomas von Zglinicki, Kenneth Rockwood, and Thomas BL Kirkwood, "Age-related frailty and its association with biological markers of ageing," *BMC medicine*, 2015, *13* (1), 1–9.

Moody, Harry R and Jennifer R Sasser, *Aging: Concepts and controversies*, Sage publications, 2020.

Murphy, Kevin M. and Robert H. Topel, "The value of health and longevity," *Journal of political Economy*, 2006, *114* (5), 871–904.

Murray, Christopher JL, Alan D Lopez, Brian Chin, Dennis Feehan, and Kenneth H Hill, "Estimation of potential global pandemic influenza mortality on the basis of vital

registry data from the 1918–20 pandemic: a quantitative analysis," *The Lancet*, 2006, *368* (9554), 2211–2218.

Nardi, Mariacristina De, Eric French, and John B Jones, "Why do the elderly save? The role of medical expenses," *Journal of political economy*, 2010, *118* (1), 39–75.

Occhino, Filippo, Kim Oosterlinck, and Eugene N White, "How occupied France financed its own exploitation in World War II," *American Economic Review*, 2007, *97* (2), 295–299.

Olshansky, S Jay, Leonard Hayflick, and Bruce A Carnes, "No truth to the fountain of youth," *Scientific American*, 2002, *286* (6), 92–95.

Palloni, Alberto and Hiram Beltrán-Sánchez, "Discrete Barker Frailty and warped mortality dynamics at older ages," *Demography*, 2017, *54* (2), 655–671.

Pascariu, Marius D and Vladimir Canudas-Romo, "Package "MortalityLaws"," 2022.

Passolt, Gregor, James J Anderson, Ting Li, David H Salinger, David J Sharrow, and Maintainer David J Sharrow, "Package "Vitality"," 2018.

Pinker, Steven, *The better angels of our nature: Why violence has declined*, Vol. 75, Viking New York, 2011.

Pompei, Francesco and Richard Wilson, "A quantitative model of cellular senescence influence on cancer and longevity," *Toxicology and industrial health*, 2002, *18* (8), 365–376.

Preston, Samuel H and Etienne Van de Walle, "Urban French mortality in the nineteenth century," *Population studies*, 1978, *32* (2), 275–297.

Preston, Samuel, Patrick Heuveline, and Michel Guillot, *Demography: measuring and modeling population processes*, Oxford: Blackwell Publishers, 2000.

Rosenberg, Karen and Wenda Trevathan, "Bipedalism and human birth: The obstetrical dilemma revisited," *Evolutionary Anthropology: Issues, News, and Reviews*, 1995, *4* (5), 161–168.

Rosenberg, Karen R, "The evolution of modern human childbirth," *American Journal of Physical Anthropology*, 1992, *35* (S15), 89–124.

Ross, Catherine E and Chia ling Wu, "The links between education and health," *American sociological review*, 1995, pp. 719–745.

Schiman, Jeffrey C, Robert Kaestner, and Anthony T Lo Sasso, "Early Childhood Health Shocks and Adult Wellbeing: Evidence from Wartime Britain," Technical Report, National Bureau of Economic Research 2017.

Schwandt, Hannes and Till M Von Wachter, "Socioeconomic decline and death: Midlife impacts of graduating in a recession," Technical Report, National Bureau of Economic Research 2020.

Schwartz, Joel, "Harvesting and long term exposure effects in the relation between air pollution and mortality," *American journal of epidemiology*, 2000, *151* (5), 440–448.

Sharrow, David J. and James J. Anderson, "Quantifying Intrinsic and Extrinsic Contributions to Human Longevity: Application of a Two-Process Vitality Model to the Human Mortality Database," *Demography*, 2016, *53* (6), 2105–2119.

Sharrow, David J, Samuel J Clark, Mark A Collinson, Kathleen Kahn, and Stephen M Tollman, "The age pattern of increases in mortality affected by HIV: Bayesian fit of the Heligman-Pollard model to data from the Agincourt HDSS field site in rural northeast South Africa," *Demographic research*, 2013, *29*, 1039.

Siler, William, "A competing-risk model for animal mortality," *Ecology*, 1979, *60* (4), 750–757.

_ , "Parameters of mortality in human populations with widely varying life spans," *Statistics in medicine*, 1983, *2* (3), 373–380.

Smith, James P., "Healthy bodies and thick wallets: the dual relation between health and economic status," *The journal of economic perspectives: a journal of the American Economic Association*, 1999, *13* (2), 144.

Steves, Claire Joanne, Timothy D Spector, and Stephen HD Jackson, "Ageing, genes, environment and epigenetics: what twin studies tell us now, and in the future," *Age and ageing*, 2012, *41* (5), 581–586.

Strittmatter, Anthony, Uwe Sunde, and Dainis Zegners, "Life cycle patterns of cognitive performance over the long run," *Proceedings of the National Academy of Sciences*, 2020, *117* (44), 27255–27261.

Strulik, Holger, "A Closed-form Solution for the Health Capital Model," *Journal of Demographic Economics*, 2015, *81* (3), 301–316.

Tanner, James Mourilyan and James Mourilyan Tanner, *A history of the study of human growth*, Cambridge University Press, 1981.

Thiele, Thorvald Nicolai, "On a mathematical formula to express the rate of mortality throughout the whole of life, tested by a series of observations made use of by the Danish Life Insurance Company of 1871," *Journal of the Institute of Actuaries*, 1871, *16* (5), 313–329.

Thomas, Duncan, Elizabeth Frankenberg, Jed Friedman, Jean-Pierre Habicht, Nathan Jones, Christopher McKelvey, Gretel Pelto, Bondan Sikoki, James P. Smith, Cecep Sumantri, and others, "Causal effect of health on labor market outcomes: Evidence from a random assignment iron supplementation intervention," *California Center for Population Research*, 2004.

Toulemon, Laurent and Magali Barbieri, "The mortality impact of the August 2003 heat wave in France: investigating the ?harvesting?effect and other long-term consequences," *Population studies*, 2008, *62* (1), 39–53.

Vaupel, James W, "Biodemography of human ageing," *Nature*, 2010, *464* (7288), 536–542.

Vaupel, James W., Kenneth G. Manton, and Eric Stallard, "The impact of heterogeneity in individual frailty on the dynamics of mortality," *Demography*, 1979, *16* (3), 439–454.

Viazzo, Pier Paolo, Carlo A Corsini et al., "The Decline of Infant Mortality in Europe, 1800-1950: Four national case studies," Technical Report 1993.

Wagstaff, Adam, "The demand for health: some new empirical evidence," *Journal of Health economics*, 1986, *5* (3), 195–233.

Weibull, Waloddi, "Wide applicability," *Journal of applied mechanics*, 1951, *103* (730), 293–297.

Wilcox, Allen J. and Ian T Russell, "Birthweight and perinatal mortality: I. On the frequency distribution of birthweight," *International Journal of Epidemiology*, 1983, *12* (3), 314–318.

Wilson, Nick, Christine Clement, Jennifer A Summers, John Bannister, and Glyn Harper, "Mortality of first world war military personnel: comparison of two military cohorts," *Bmj*, 2014, *349*, g7168.

Wong, Chloe Chung Yi, Avshalom Caspi, Benjamin Williams, Ian W Craig, Renate Houts, Antony Ambler, Terrie E Moffitt, and Jonathan Mill, "A longitudinal study of epigenetic variation in twins," *Epigenetics*, 2010, *5* (6), 516–526.

Zeger, Scott L, Francesca Dominici, and Jonathan Samet, "Harvesting-resistant estimates of air pollution effects on mortality," *Epidemiology*, 1999, pp. 171–175.

Figures

Figure 1: Cohort Mortality rates for Selected European Cohorts born 1860 -1940

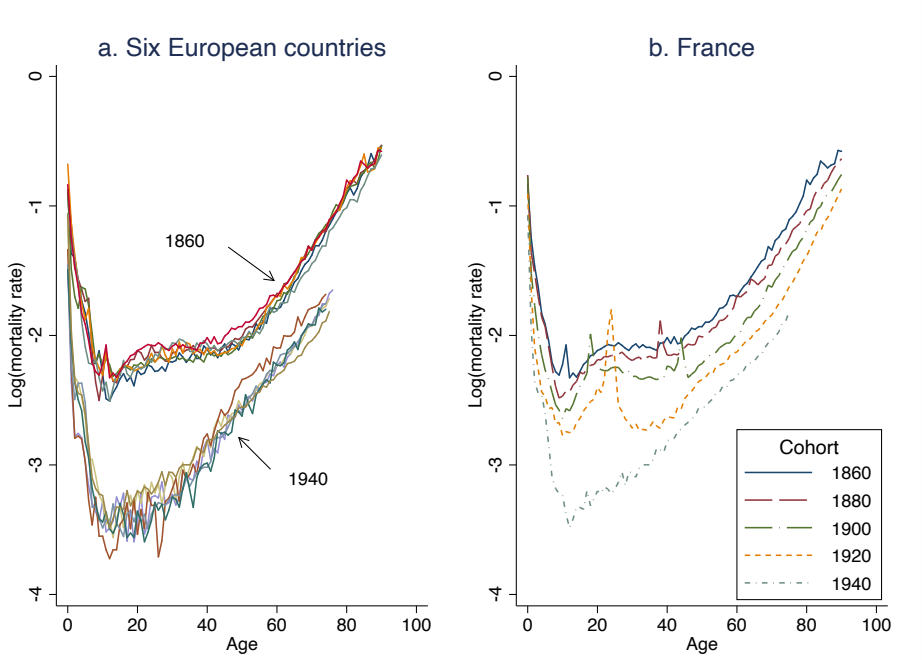

Note: Human Mortality Database. *Panel a* shows the $\log_{10}$ of the mortality rates by age for women born in 1860 and in 1940, in six European countries (Belgium, Denmark, the Netherlands, Sweden, France, and Norway). *Panel b* shows the mortality rates for women born in France in 1860, 1880, 1900, 1920 and 1940.

Figure 2: Health and mortality in the first two years of life

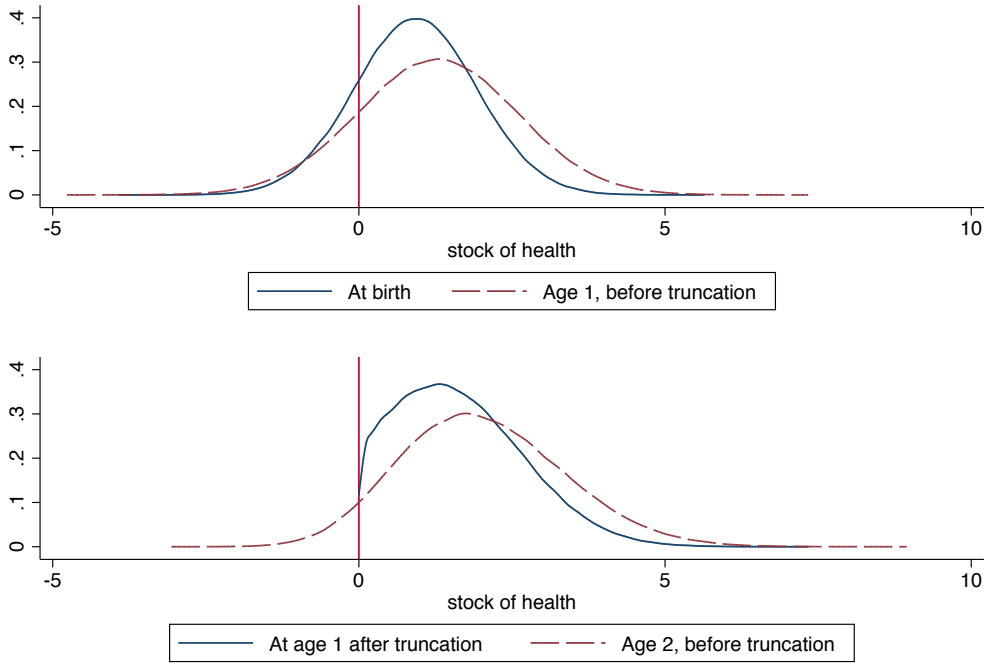

Data from simulations

The figure shows the evolution of the distribution of health in the first two periods of life in a population where I exceeds the force of aging δa^{α} in the first two periods.

Figure 3: Model behavior

(a) The evolution of the health distribution over the lifetime

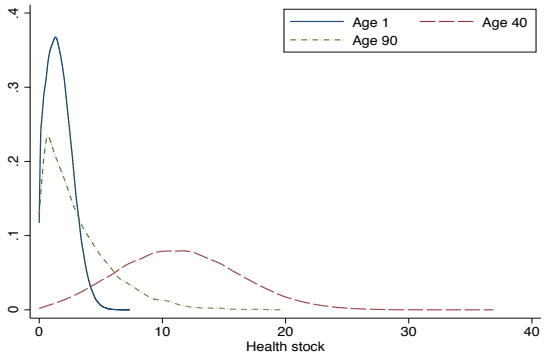

(b) Age profile of population health and mortality without external causes of death (adolescent hump)

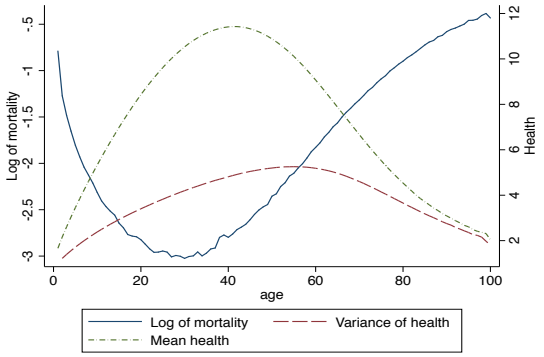

Note: Simulated data for a population of 500,000 individuals and without adolescent bump. For this simulation we use the following parameters: I=0.3575753, δ=0.0004789, σ=0.8353752, α=1.7883, μ_0=0.925079. *Panel a* shows the density of health for the population at ages 1, 40 and 90. *Panel b* plots the average health, the variance of health and the mortality rates of the population over the lifetime.

Figure 4: Adding accidents to the baseline model

(a) Adding accidents to the model

(b) US Mortality rates per 1,000 in 1990, by cause of death

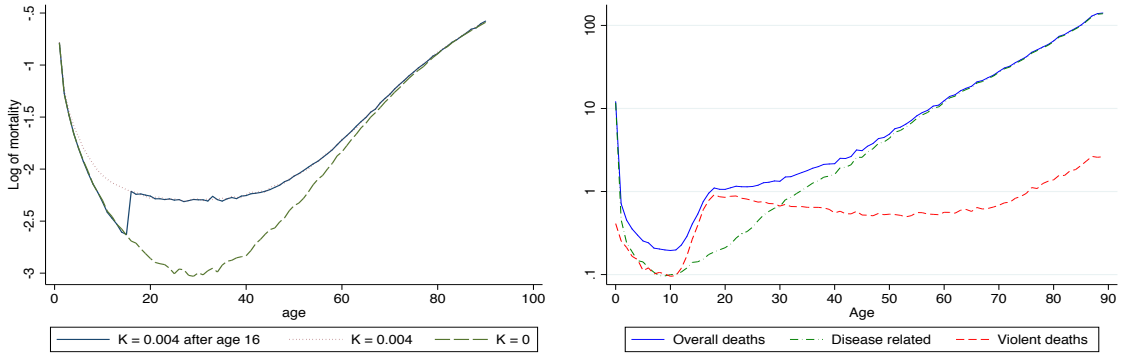

Note: *Panel a* shows the evolution of mortality based on a simulation that uses the same baseline parameters as in Figure 3. The green dashed line shows the mortality curve without any accidents ($\kappa = 0$). The red dotted line shows the mortality curve of a population that experiences a $\kappa = 0.004$ percent chance of dying every period due to an accident, unrelated to health. The blue line shows the model which assumes the accident rate is zero at birth but jumps to 0.004 in adolescence. Mortality rates are higher as a result of external deaths but more among young adults because of competing risks: older individuals that are hit by an accident shock are also unhealthy and would die even in the absence of an accident shock. *Panel b* is reproduced from Schwandt and Von Wachter (2020) who generously agreed to let us use it. The data come from *period* (not cohort tables) so they are not directly comparable to ours. But we use it to demonstrate that the mortality rate from non-disease related causes of death is well approximated by a step function that turns on in adolescence. Mortality rates are shown in log(10) scale.

Figure 5: Evolution of survival for French females born 1816-1940

(a) French women born in 1816

(b) Observed and Estimated Cohort Survival Rates

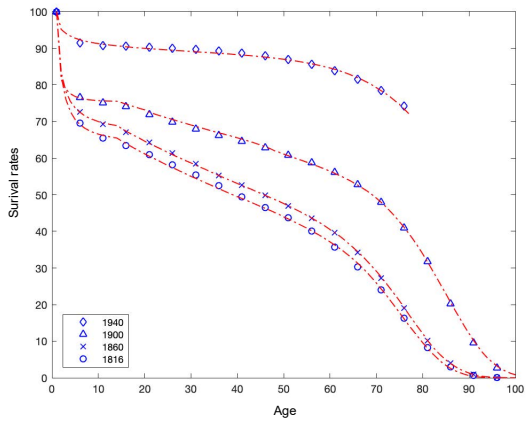

(c) Evolution of health at birth (μ_o) across cohorts

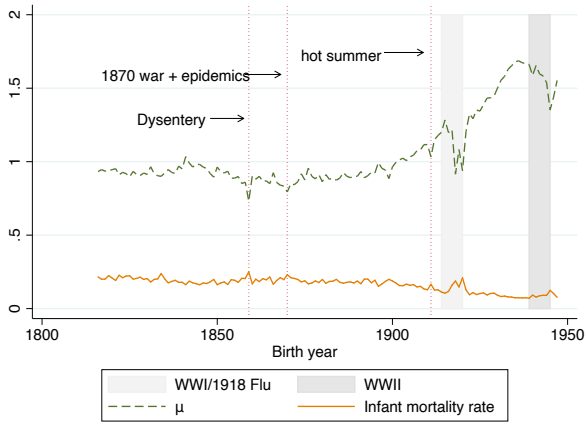

(d) Estimated external causes of death across cohorts

(e) Force of aging

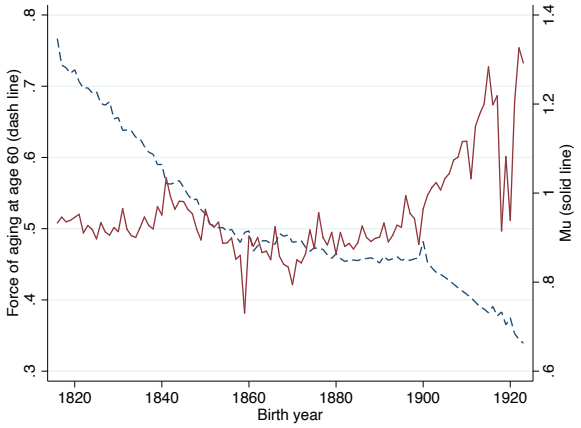

(f) Decrease in (I) during WWI/1918 pandemic

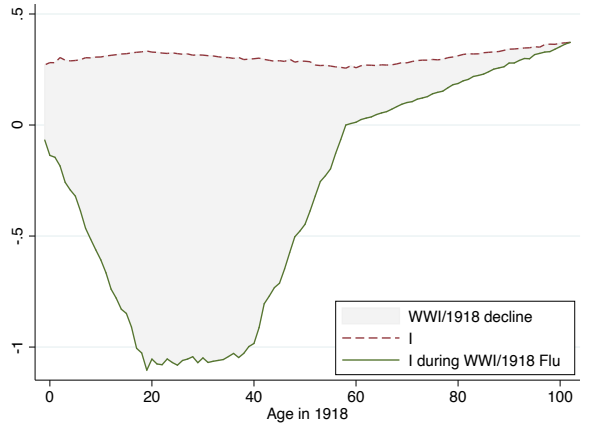

Note: *Panel a* shows the observed mortality rates and the predicted rates for French women born in 1816. *Panel b* shows the observed (blue markers) and estimated (red dashes) survival curves for four cohorts of French women. *Panel c* shows the evolution of the infant mortality rate and μ_0. *Panel d* shows the estimates of mortality from external causes (κ) alongside the average probability of dying across ages 15 to 24 (from cohort tables). *Panel e* shows the estimated function of aging at age 60, as $\delta(60)^{\alpha}$ and μ_o. *Panel f* shows the estimated effect of the WWI/1918 on I as a function of the age on the onset of the shock.

Figure 6: Generating SES gradients in health and mortality

(a) Persistent SES Mortality gap in our model

(b) Persistent SES Mortality gap in Chetty et al. (2016)

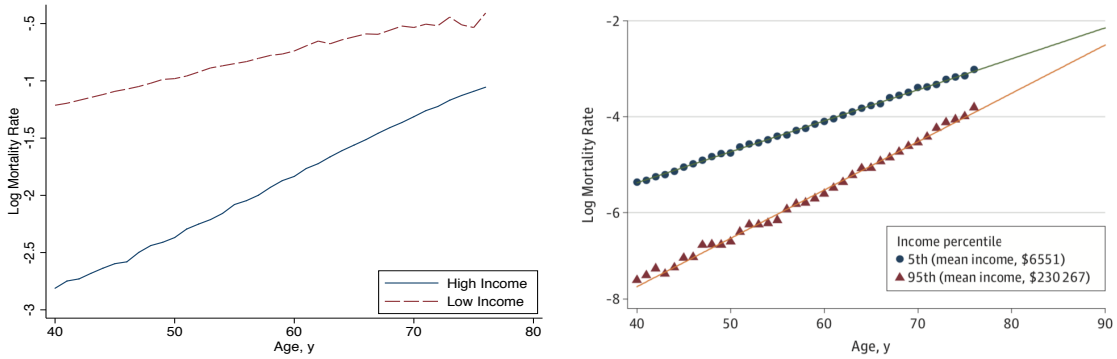

(c) Lifetime SES gaps in mortality

(d) Lifetime SES gaps in health

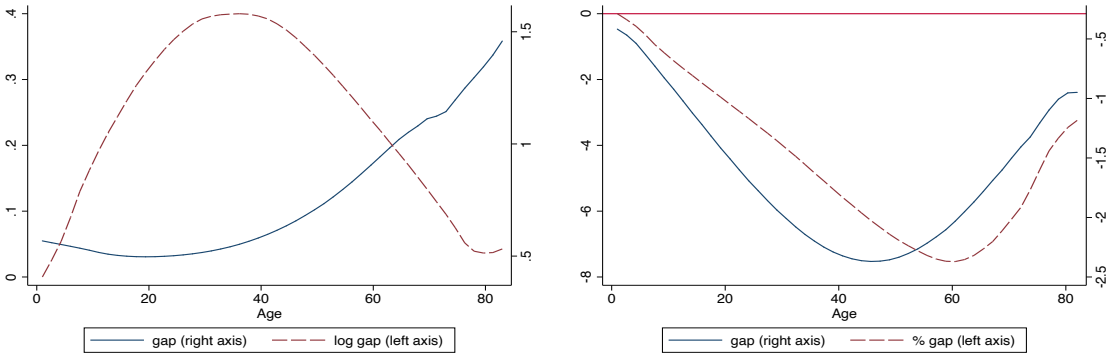

Note: *Panel a* shows the predicted mortality rate for the 1816 cohort (using the parameters from in Appendix Table 1 but setting the accident rate at 0 throughout for simplicity) and the counterfactual mortality that results from a 95% decline in I for this population. The baseline 1816 cohort is labeled "High Income" and the counterfactual population is labeled "Low Income." *Panel b* reproduces the results from Chetty et al. (2016) and shows the mortality rates of high and low income populations in the US. *Panel c* shows the simulated effects of decreasing the baseline level of I (our proxy for SES) by 50% on mortality in both levels and percentage terms. We plot the gap between the baseline and the affected population. This gap is computed as MR(low SES)-MR(high SES). *Panel d* shows the effects of increasing the baseline level of I by 50% on health. This gap is computed as H(low SES)-H(high SES). The baseline parameters are the same as in Figure 3.

Figure 7: The effects of negative in-utero shocks

(a) Monotonic effects in Grossman's model

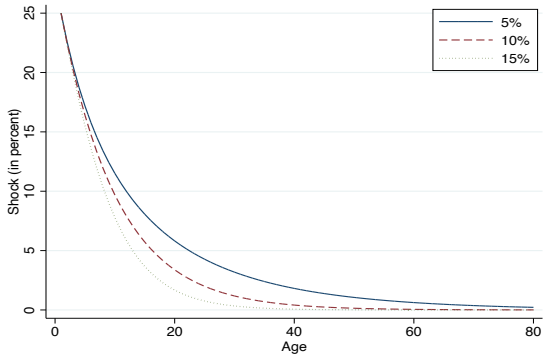

(b) U-shaped decreases in health in our model

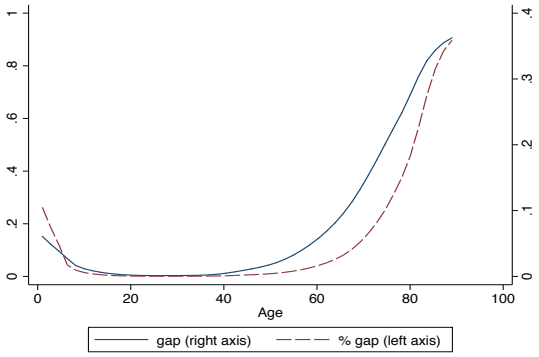

(c) Negative in-utero shocks increase lifetime mortality

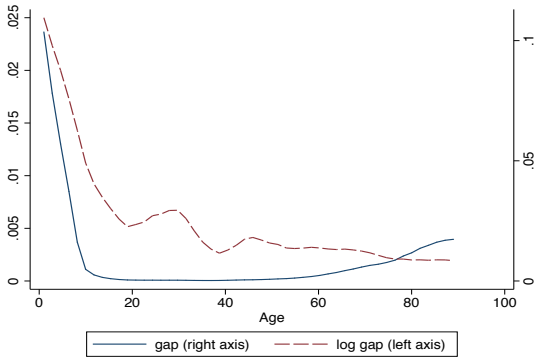

Note: *Panel a* reproduces and extends the figure in Almond and Currie (2011) and shows the decline in the health stock due to a 25% shock in utero that is predicted by the standard Grossman model. We simulate the evolution of health for two populations using Grossman's equation for the evolution of health (also eq. 1 of Almond and Currie, 2011) which states that $H_t = (1-\delta)H_t + I_t$. We set $\mu_0 = 10$ for one population and $\mu_0 = 7.5$ for the shocked population; and we set $I = 1$ for both. The figure reports the differences in H by age, expressed in percentage terms relative to the baseline population. This effect is initially large but it fades over time and will be close to zero among adults older than 30, though the extent of this fade out depends on the level of depreciation rate which we set at 5, 10 and 15%. *Panel b* shows the simulated effects of a 50% decline in in-utero health for the 1816 French population in our model (setting the accident rate at 0 throughout for simplicity). The figure plots the decreases in health, in either levels or percentage terms. In contrast to the Grossman model our model predicts a U-shape pattern of effects: high in childhood, low in middle age and increasing among the old. *Panel c* shows the effects on mortality of a 50% decline in in-utero health in both levels and percentage terms. The figure shows mortality increases as a result, and the age pattern of the effects varies depending on whether we express them in levels or logs. The baseline parameters used on panels b and c are the same as in Figure 3.

Figure 8: Scarring and Harvesting effects

(a) Scarring effects of WWI on the mortality rates of French men born in 1896

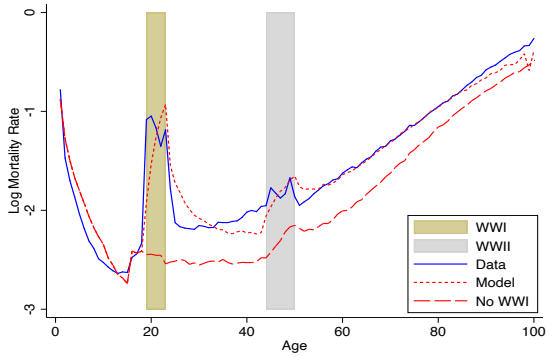

(b) Harvesting in the model among the old

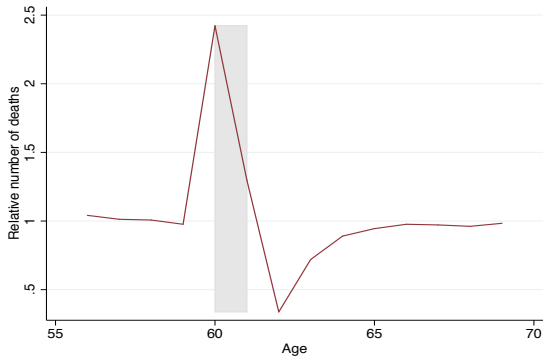

Note: *Panel a* shows the scarring effect on mortality rates of WWI for men born in France in 1896 who turned 18 when WWI started in 1914 and who would have served in the military. The blue solid line shows the observed mortality rates for this cohort. The dotted red line shows the predicted mortality rates, that result from estimating the model and including one more parameter for WWI and another for WWII. We allow for I to be different during each war. The counterfactual curves (dashed red lines) show what the mortality curves would look like in the absence of WWI by predicting that the rates would have been in the absence of a decline in I during WWI. *Panel b* shows the simulated effects of a temporary increase in the threshold (from 0 to 0.8) at ages 60 and 61 on the 1816 French cohort (setting the accident rate to 0 for simplicity). The y-axis plots the relative number of deaths in the affected population divided by the number of deaths in the unaffected population. The figure shows that deaths get shifted earlier. This displacement is estimated to result in approximately 8,000 excess deaths during the shock and fewer deaths for the subsequent 2 years.

Appendix A: Figures & Tables

Figure 9: Comparison of q-rate in the paper and in the HMD (1816)

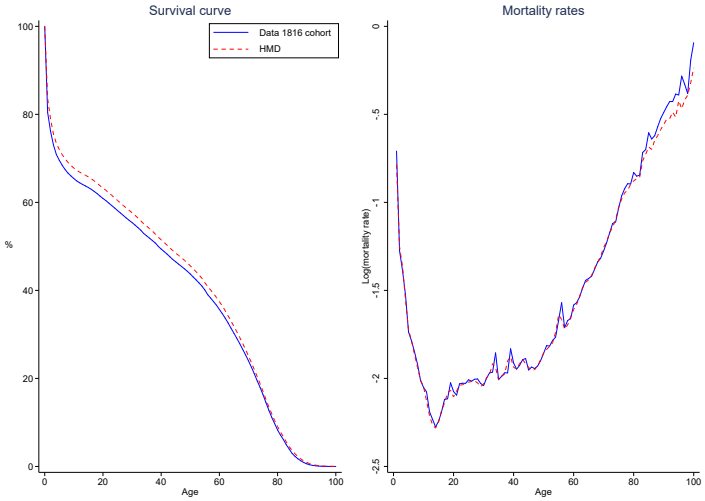

Note: The life expectancy is 38.25 years with the q we use (see Appendix D), to be compared with 39.86 with the q in HMD and 39.83 years for the life expectancy computed by the HMD itself following a more involved statistical methodology.

Figure 10: Cohort vs. Period statistics, French Women 1860 and 1940

(a) Cohort vs Period Life Expectancy for French Females

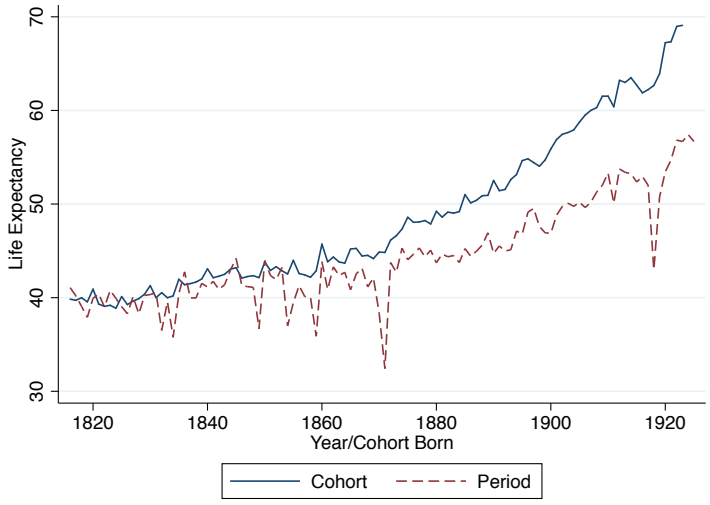

(b) Cohort vs Period Life Expectancy for French Males

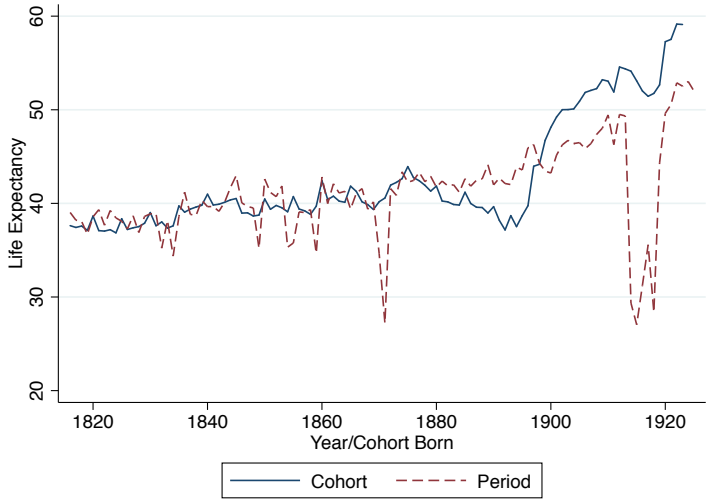

Note: Data from the Human Mortality Database. *Panel a* shows that period and cohort life expectancy for French females were almost identical for the cohort borns before 1860, suggesting that for these cohorts the assumption of stationarity holds, but starting sometime in the late 19th century the curves diverge and cohort life expectancy exceeds period life expectancy substantially. This occurs because the period life expectancy overestimates the mortality rates that the cohort will experience at older ages due to improvements in mortality. *Panel b* shows the period and cohort life expectancy of French men since 1816. The two series are almost the same up to roughly 1880 and they diverge after, with the cohort life expectancy exceeding the period life expectancy substantially by the end of the period. For men the cohort life expectancy does not rise monotonically. We observe that actual (cohort) life expectancy is lower than predicted (period) life expectancy for cohorts born between 1880 and 1900, likely as a result of WWI and WWII.

Figure 11: Age profile of mortality of women born in France between 1860 and 1940, by decade

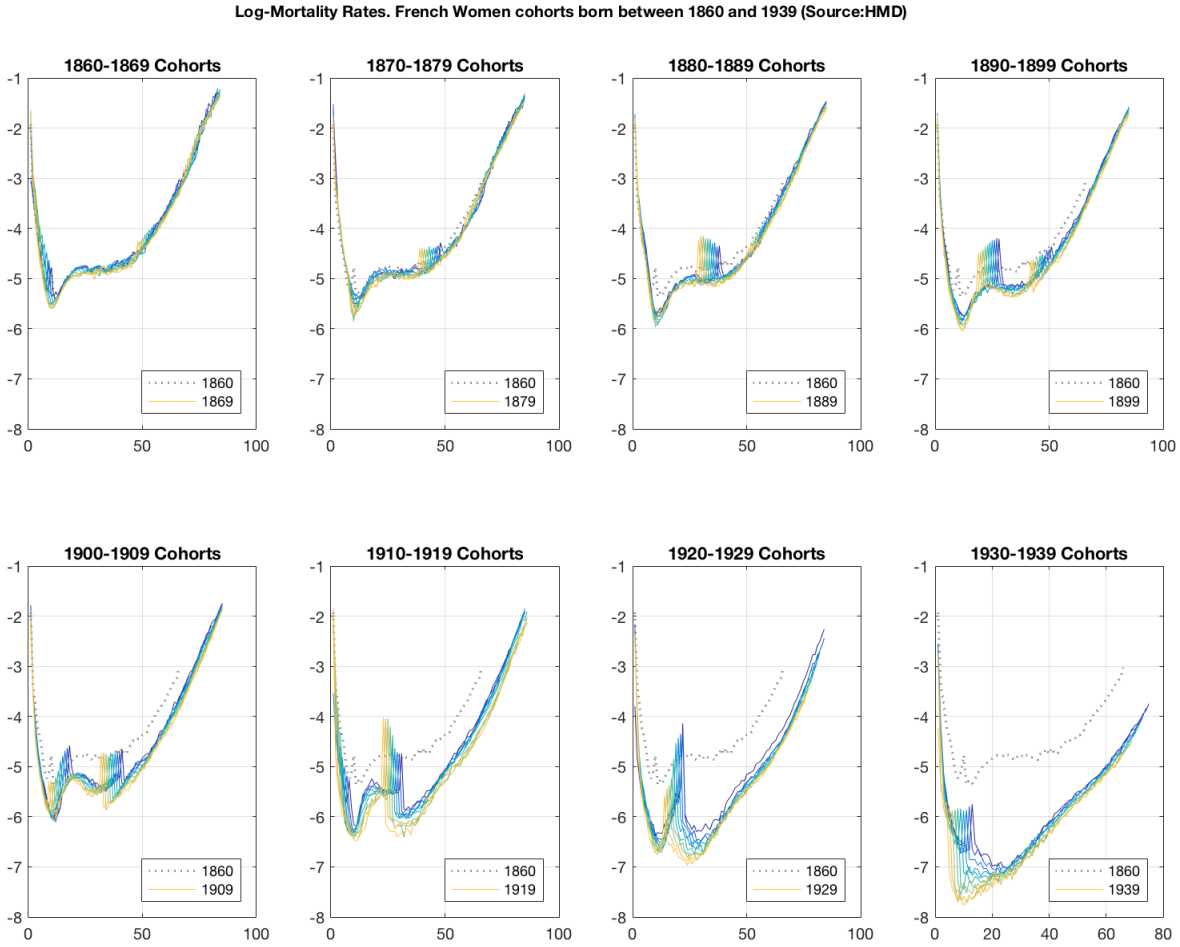

Note: Human Mortality Data

Figure 12: Age profile of mortality of men born in France between 1860 and 1940, by decade

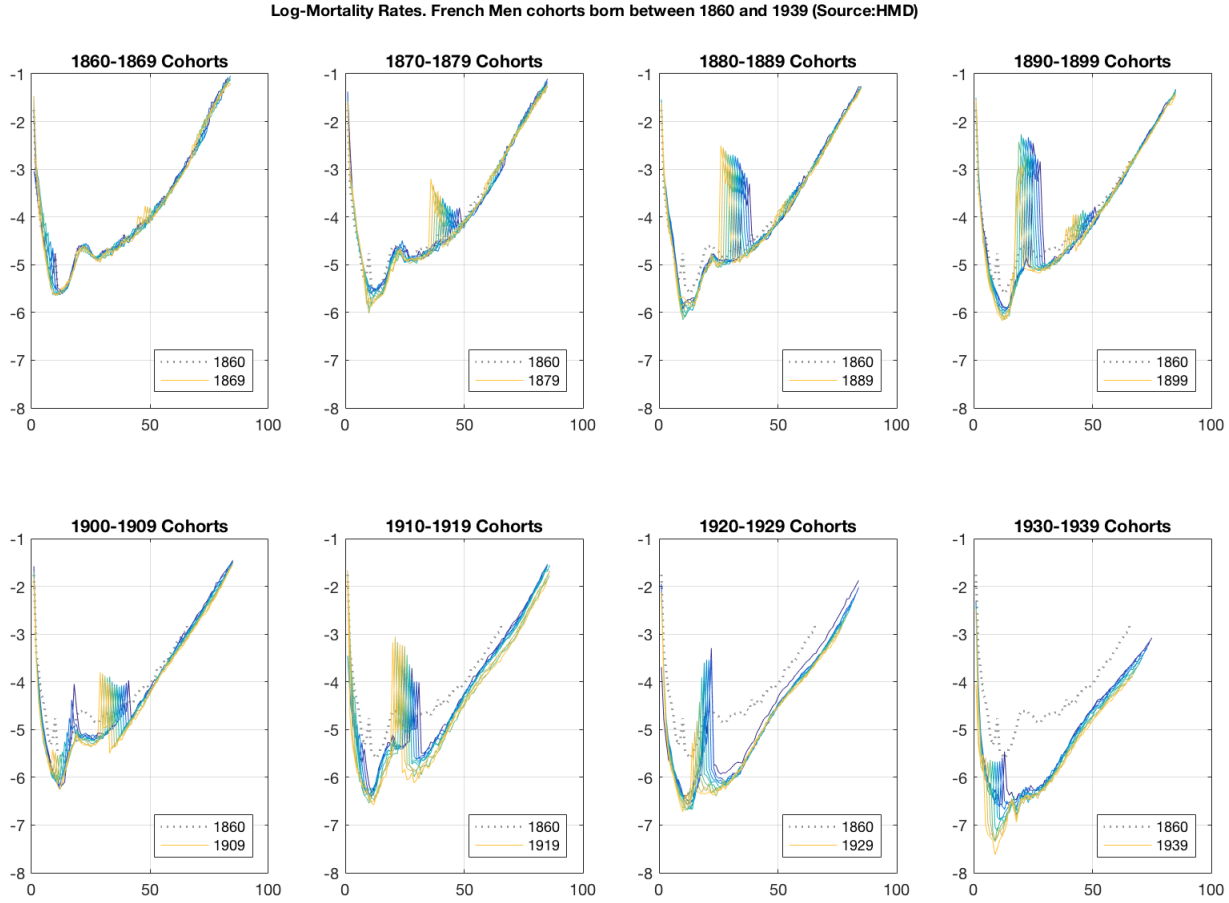

Note: Human Mortality Data

Figure 13: Model fit for humans and primates

(a) French men born in 1816

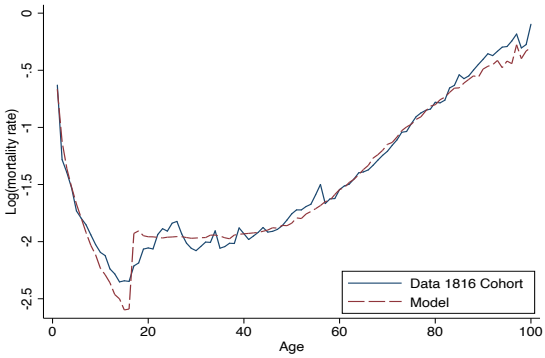

(b) Female chimpanzees

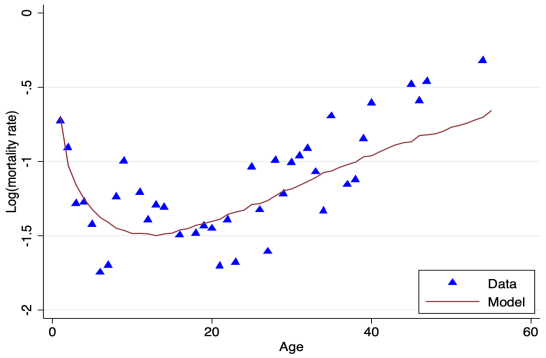

(c) Male chimpanzees

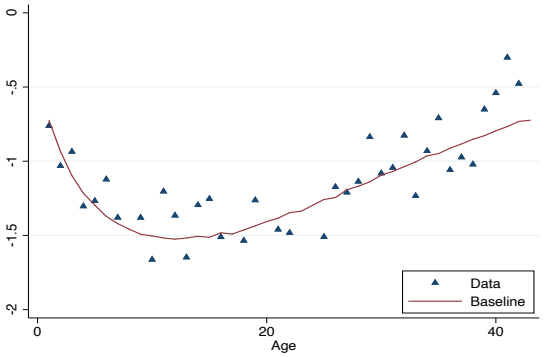

Note: *Panel a* shows the observed and predicted mortality rates for French men born in 1816. Appendix Table 1 show the estimated parameters for men. *Panel b* shows the data and estimated mortality rates for female chimps. *Panel c* shows the data and estimated mortality for male chimps. Appendix Table 3 show the estimated parameters for chimps.

Figure 14: Health Resources and Variance of Health Resources

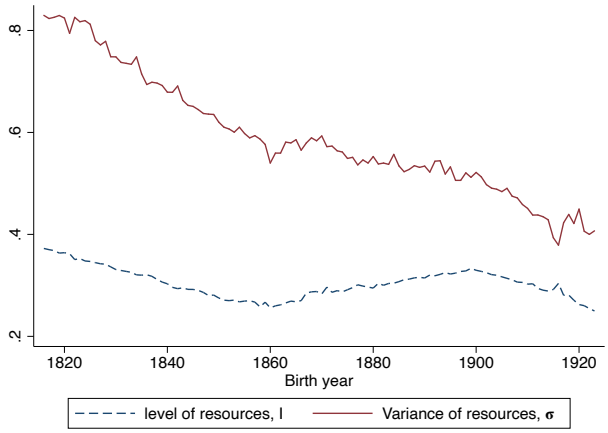

Note: Figure shows the estimates for I and σ, the level of health resources and its variance for all cohorts.

Figure 15: Model fit for birth cohorts born 1816-1923

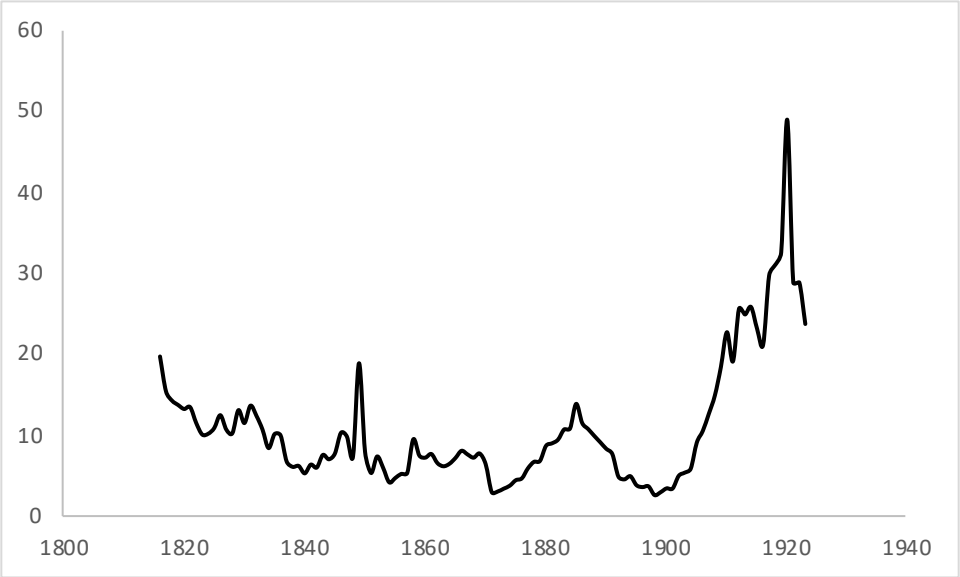

Note: this figure shows the fit of the model for each birth cohort. The fit is measured as the sum of quadratic errors between the estimated survival curve and the data at each age, defined as $\sum_a \left(\hat{S}_a - S_a\right)^2$. A lower number indicates a greater fit (smaller errors).

Figure 16: Increasing the lifetime depreciation rate by 50% by age

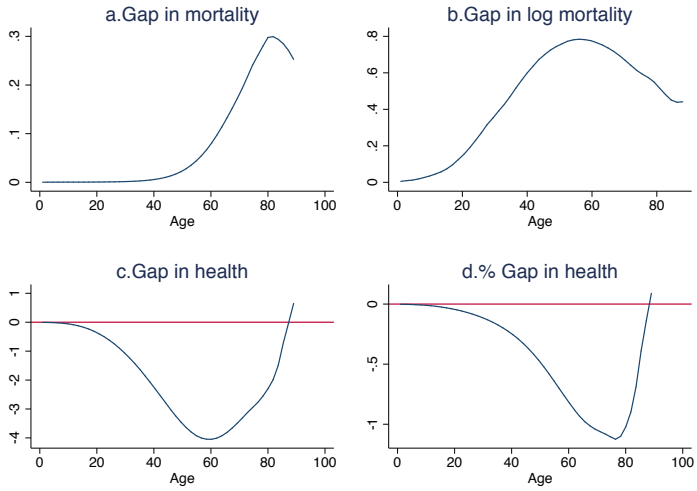

Note: The Figure shows the gap in mortality or health between a baseline population and a population with a 50% higher depreciation rate δ. Gap is computed as MR(low)-MR(high), or H(low)-H(high). The figures become very noisy after age 90 because there are almost no survivors, so we do not include these data points. Simulated data for two population of 500,000 individuals each. The baseline parameters are the same as in Figure 3.

Figure 17: The effects of temporary increases in the threshold

(a) Harvesting during the French 2003 Heatwave

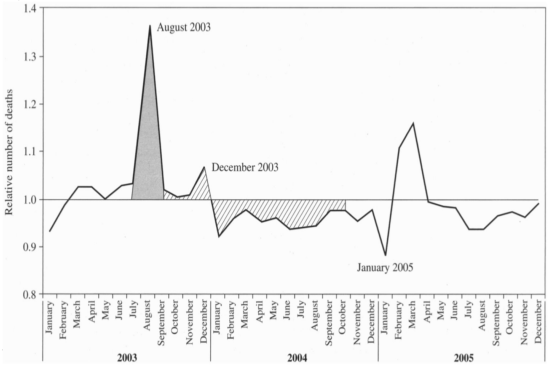

(b) Harvesting in the model among the old

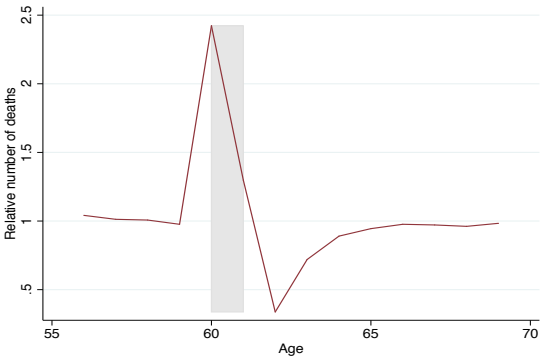

(c) Harvesting in the model among the young

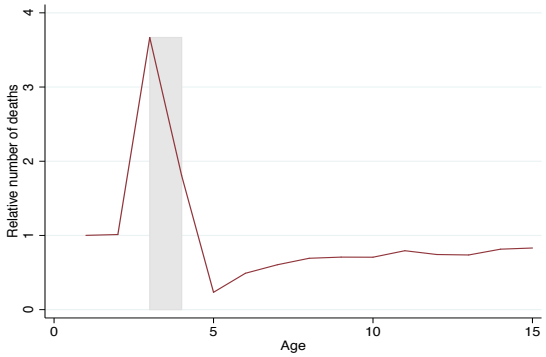

Note: *Panel a* is reproduced from Toulemon and Barbieri (2008) and shows the mortality displacement created by the French 2003 Heatwave. The number of excess deaths in Summer 2003 is computed relative to the number of deaths during the same period in 2000. The grey (hatched) area corresponds to an excess (deficit) of 15,000 deaths. These excess deaths are computed for the entire population. *Panel b* shows the simulated effects of a temporary increase in the threshold (from 0 to 0.8) at ages 60 and 61 on the 1816 French cohort (setting the accident rate to 0 for simplicity and using the parameters from Figure 3) which results in approximately 8,000 excess deaths during the shock and fewer deaths for the subsequent 2 years. *Panel c* shows the simulated effects of a temporary increase in the threshold (from 0 to 0.8) at ages 3 and 4 on the 1816 French cohort (setting the accident rate to 0 for simplicity) which results in approximately 40,000 excess deaths during the shock. The effect is much larger among the young because many more children are close to the threshold as shown in Figure 3a. But the displacement effect is spread out over a much longer period for children.

Figure 18: Effects of temporary shocks on log mortality rates

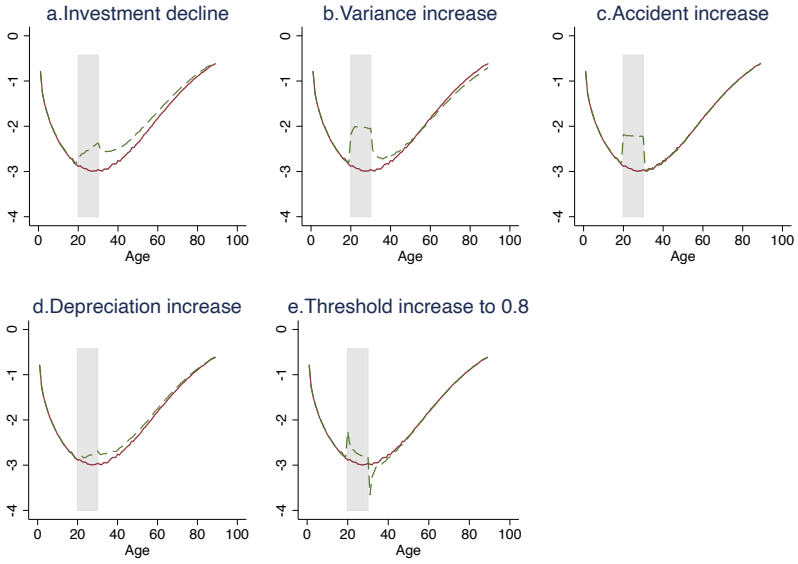

Note: Results from simulations using the 1816 cohort parameters and assuming no adolescent hump. Shocks correspond to a 50% change in the parameter, except for the threshold, which is assumed to increase to 0.8 from 0. The shock starts at age 20 and lasts 10 years, ending at age 30.

Figure 19: Effect of exogenous temporary shocks at age 20

(a) Gaps in mortality

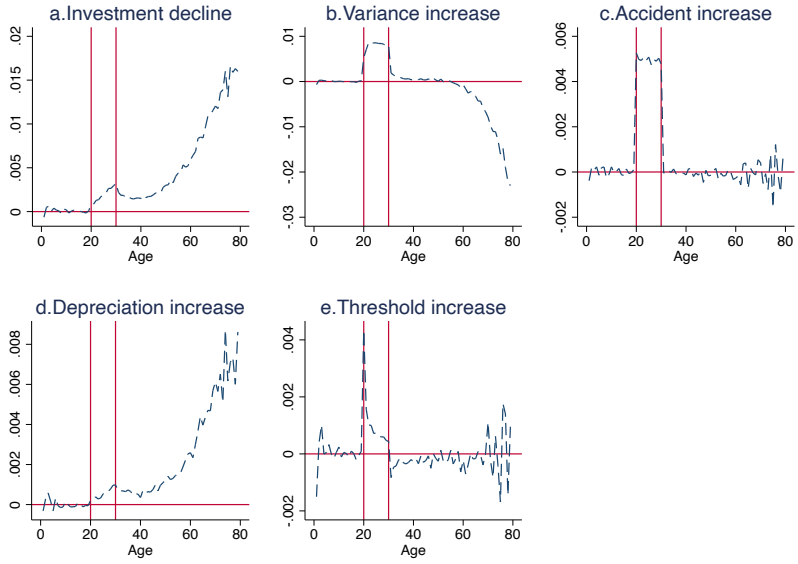

(b) Gaps in log mortality

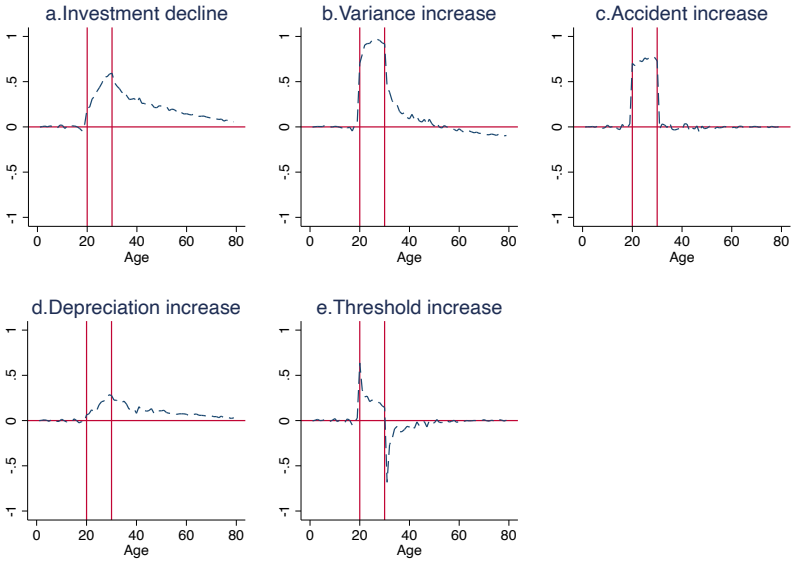

Note: The figure shows the effects of a temporary change in a single parameter occurring at age 20 in a simple model without adolescent humps. The shock lasts for 10 years, ending at age 30. Each figure shows the different in mortality that results from a temporary shock, relative to the counterfactual of no shock. In essence these figures plot the pattern that would be predicted in an event study, where the coefficient of a dummy for the affected population is interacted with time fixed effects. *Panel a* shows the gaps in levels and *panel b* shows the gaps in logs. The gaps in levels are not shown in the same scale to make the patterns more apparent. The baseline parameters are the same as in Figure 3.

Figure 20: Effects of exogenous permanent shocks at age 20

(a) Gaps in mortality

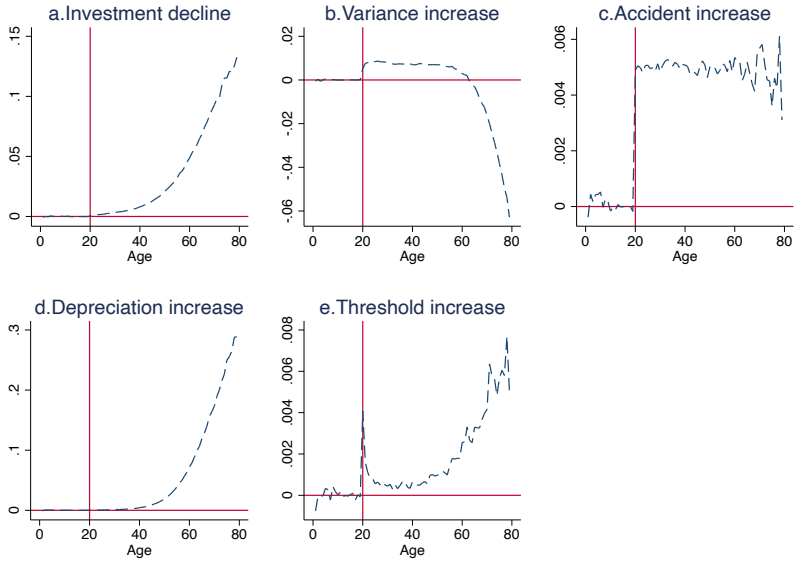

(b) Gaps in log mortality

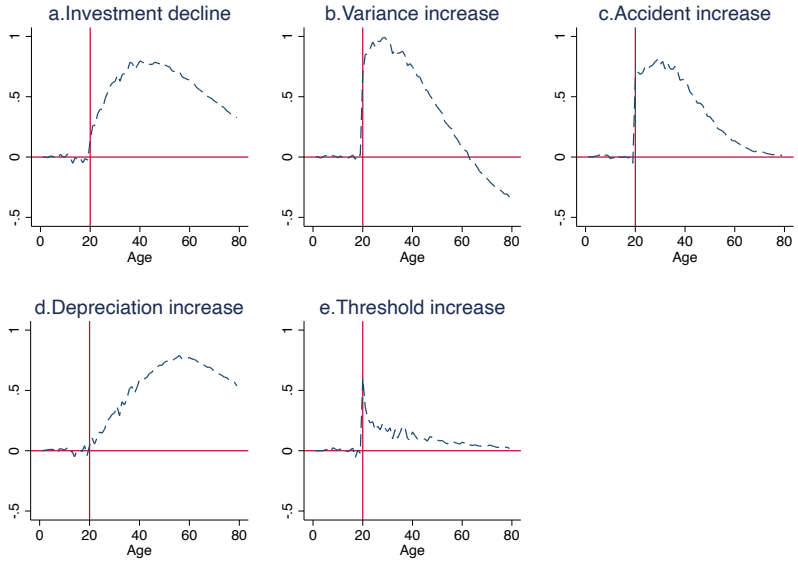

Note: The figure shows the effects of a permanent change in a single parameter occurring at age 20 in a simple model without adolescent humps. Each figure shows the different in mortality that results from a temporary shock, relative to the counterfactual of no shock. In essence these figures plot the pattern that would be predicted in an event study, where the coefficient of a dummy for the affected population is interacted with time fixed effects. *Panel a* shows the gaps in levels and *panel b* shows the gaps in logs. The gaps in levels are not shown in the same scale to make the patterns more apparent. The baseline parameters are the same as in Figure 3.

Figure 21: Optimal Investment Levels by Age

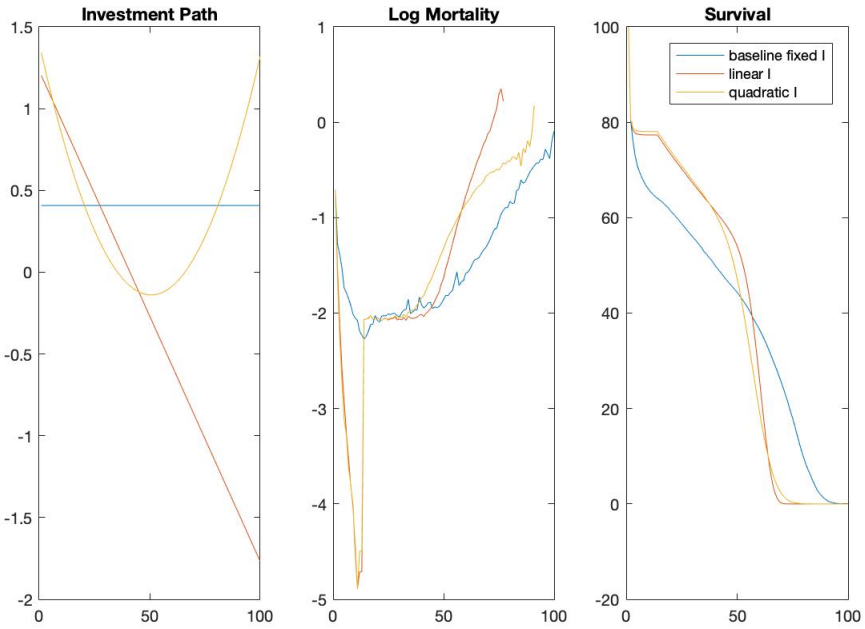

Note: The first panel represents the estimated investment path when investment is constrained to be constant (blue line), linear (red line), or quadratic (yellow). In the second and third panel, 1816 cohort data is represented in blue. Both linear and quadratic optimal investment paths would devote more resources to younger cohorts, reducing mortality rates in the early years.

Table 1: Modeling prime-age mortality. French Cohort born in 1816

		(1)	(2)	(3)	(4)
Gender		Females		Males	
Model		Baseline	With adolescent hump	Baseline	With adolescent hump
Initial mean health	μ_H	0.9115	0.8634	0.7091	0.7104
Investment	I	0.1336	0.4075	0.1209	0.4432
Standard Deviation of Shock	σ_e	0.5556	1.0241	0.4700	1.0785
Depreciation	δ	0.0010	0.0006	0.0014	0.0004
Aging	α	1.4350	1.7849	1.3182	1.8883
Adolescent Hump*	κ		0.0086		0.0097
Fit (survival curve)^		155.06	12.36	143.07	16.38
Fit (log of q_x)		3.01	0.74	4.02	0.91
Fit (death distribution)**		6.21	3.35	18.10	96.16
Actual Life Expectancy		38.25	38.25	35.93	35.93
Predicted Life Expectancy		38.43	38.28	36.13	35.94
Counterfactual Life Expectancy^^			45.86		43.54

Note: In this table, we fit the model to the 1816 population with and without an exogenous increase in the accident rate occurring in adolescence.

*The estimate in this row corresponds to the value of the parameter κ after the onset of adolescence. Adolescence starts at age = (- 0.0175 x calendar year) + 47.4 for all women, based on the estimates provided in de La Rochebrochard (2000). Adolescence starts one year later for men.

^Our main fit criteria is the sum of squared errors of the survival rate at each age. We also report the fit as the sum of squared errors of the log of q_x (the probability of dying between ages x and $x+1$) and the distribution of deaths. We don't target these moments directly–we target the survival curve.

**To make the fit of the age distribution comparable across columns we use the (normalized) number of deaths as weights.

^^Counterfactual Life Expectancy is computed by holding all estimated parameters fixed and setting the adolescent hump to 0.

Table 2: Robustness checks for 1816

		(1)	(2)	(3)	(4)	(5)	(6)	(7)
		Basic	κ_b	κ_b at $T \sim N()$	$N()$ estimated	Weight	Target death	Truncation at 90
Initial mean health	μ_H	0.8634	0.8917	0.8635	0.7503	0.8020	0.7327	0.8784
Investment	I	0.4075	0.4322	0.4149	0.3712	0.4180	0.4743	0.4200
Standard Deviation of Shock	σ_e	1.0241	1.0713	1.0367	0.8369	0.9971	0.9930	1.0552
Depreciation	δ	0.0006	0.0005	0.0005	0.0005	0.0006	0.0006	0.0006
Aging	α	1.7849	1.8321	1.8153	1.8011	1.7807	1.7950	1.7973
Adolescent Hump*	κ_a	0.0086	0.0089	0.0089	0.0112	0.0093	0.0108	0.0087
Accident rate before adolescence	κ_b		0.0005					
Mean*				15.6	14.29			
Standard deviation*				1.32	15.71			
Fit (survival curve)^		12.36	13.03	11.49	3.75	15.86	173.74	12.36
Fit (log of q_x)		0.74	0.65	0.57	0.40	0.92	1.93	0.56
Fit (death distribution)**		3.35	39.55	21.82	2.25	6.89	4.48	28.17
Actual Life Expectancy					38.25			
Predicted Life Expectancy		38.28	38.29	38.28	38.26	38.33	39.27	38.27
Counterfactual Life expectancy^^		45.86	46.45	46.08	48.82	46.66	49.49	45.86

*Adolescence starts at age = (- 0.0175 x calendar year) + 47.4 in columns 1, 2, 5, 6 and 7. *In column 1* we estimate the basic model. *In column 2* we allow for the mortality from external causes of death before adolescence to be estimated (we do not set it to 0). *In column 3* the timing of adolescence is assumed to follow a normal distribution with mean value (- 0.0175 x calendar year) + 47.4, and standard deviation 1.3285, calculated from the table of 1975 girls in de La Rochebrochard (2000). *In column 4* we estimate the mean and the standard deviation of the onset of adolescence. *In column 5* we investigate what happens if we use the (normalized) number of deaths as weights in the estimation. *In column 6* we use weights and target the distribution of the ages at death instead of the survival curve. *In column 7* we use only data up to age 90 to see what the effect of censoring is and because the data after 90 are estimated.

^Our main fit criteria is the sum of squared errors of the survival rate at each age. We also report the fit as the sum of squared errors of the log of q_x (the probability of dying between ages x and $x+1$) and the distribution of deaths. We don't target these moments directly–we target the survival curve.

^^Counterfactual Life Expectancy is computed by holding all estimated parameters fixed and setting the adolescent hump to 0.

**To make the fit of the age distribution comparable across columns we use the (normalized) number of deaths as weights.

Table 3: Estimated parameters for chimpanzees living in the wild

		(1)	(2)	(3)	(4)	(5)	(6)
Gender		Female			Male		
Model		Basic model	Hump at 8	Hump at 14	Basic model	Hump at 8	Hump at 14
Initial mean health	μ_H	0.9995	1.0337	1.0266	1.8421	3.6402	4.5330
Investment (annual)	I	0.3488	0.3613	0.3603	0.7646	1.1364	0.7353
Standard Deviation of Shock	σ_e	1.1299	1.1806	1.1787	2.7145	4.9725	5.0730
Depreciation	δ	0.0598	0.0600	0.0593	0.0620	0.0510	0.0073
Aging	α	0.7627	0.7736	0.7763	1.0319	1.2501	1.8028
Adolescent Hump*	κ		0.000040	0.000002		0.000378	0.000003
# of individuals at birth		144	144	144	122	122	122
# of moments reported		55	55	55	43	43	43
Fit (survival curve)^b		111.12	110.20	110.25	128.43	99.26	65.63
Fit (log of q_x)		2.08	2.07	2.09	1.21	1.14	1.06
Actual Life Expectancy		15.38$(13.4)^a$	15.38$(13.4)^a$	15.38$(13.4)^a$	14.47	14.47	14.47
Predicted Life Expectancy		15.35	15.35	15.35	14.52	14.50	14.50

Columns (1) and (4) estimate the model without an adolescent hump. Columns (2) and (4) estimate the model with an exogenous increase in accidents in adolescence at age 8. Columns (3) and (6) estimate the model with an exogenous increase in accidents in adolescence at age 14. Because the data are noisy the second/third model is not a substantially better fit than the first. All are however excellent fits for this population.

Data sources: Life tables for primates in the wild come from Bronikowski et al. (2011). The wild population data come from Brazil, Costa Rica, Kenya, Tanzania, Madagascar and Rwanda.

a. Life expectancy in parenthesis corresponds to the one reported in Bronikowski et al. (2011).

b. We target the survival curve and compute the sum of squared errors – the data provided are in the form of survival rates.

*Adolescence starts at age 8.

Table 4: Estimated parameters for French Women and Men for Selected Cohorts

Gender		Females					Males				
Year		1816	1860	1880	1900	1921	1816	1860	1880	1900	1921
Initial mean health	μ_H	0.9327	0.9034	0.8633	0.9643	1.2051	0.7038	0.7848	0.5812	0.6747	1.0929
Investment	I	0.3724	0.2559	0.2947	0.3296	0.2602	0.4083	0.2455	0.3386	0.4711	0.2483
Standard Deviation of Shock	σ_e	0.8296	0.5400	0.5527	0.5215	0.4062	1.0120	0.6200	0.6705	0.8235	0.5067
Depreciation	δ	0.0005	0.0006	0.0006	0.0006	0.0008	0.0005	0.0006	0.0006	0.0004	0.0009
Aging	α	1.7916	1.6411	1.6248	1.6337	1.4870	1.8048	1.6587	1.6603	1.8540	1.4844
Adolescent Hump*	κ	0.0094	0.0077	0.0069	0.0050	0.0022	0.0092	0.0075	0.0079	0.0059	0.0030
I during WWI/Flu**		0.3722	0.0000	-1.0284	-1.0266			0.1926	-0.6931	-0.0313	
I during WWII**			0.2555	0.1035	0.0002	-0.0660		0.0698	0.3101	-0.2086	0.0021

*The estimates in this row correspond to the value of the parameter κ after the onset of adolescence. Adolescence starts at age = (- 0.0175 x calendar year) + 47.4 for all women, based on the estimates provided in de La Rochebrochard (2000) about the onset of menarche for girls. Adolescence starts one year later for men.

**The estimates in this row correspond to the value of the parameter during the world wars. For example the column for the 1900 female cohort shows that I was about 0.3296 throughout life but decreased to -1.02 during WWI and to 0.0002 during WWII.

Table 5: Estimated parameters for World Wars for French Men born in 1896

		(1)	(2)
Initial condition	μ_H	1.1417	0.8448
Investment	I	0.4548	0.3009
Standard Deviation of Shock	σ_e	1.0259	0.5983
Depreciation	δ	0.0002	0.0005
Aging	α	2.0052	1.6913
Adolescence Hump*	κ	0.0025	0.0037
WWI Shock**		-1.3104	
Shock in 1914			-2.9302
Shock in 1915			-0.7485
Shock in 1916			-0.5333
Shock in 1917			0.2570
Shock in 1918			-0.1191
WWII Shock**		0.0577	0.1560
Fit (survival curve)^		218.64	11.57
Fit (log of q_x)		2.65	1.27
Fit during WWI (log of q_x)~		1.09	0.09
% Difference in # deaths during WWI~~		-0.14	-0.05
Fit during WWII (log of q_x)~		0.10	0.09
% Difference in # deaths during WWII~~		0.02	-0.11
Actual Life Expectancy		37.94	
Predicted Life Expectancy		37.98	37.96
Counterfactual Life Expectancy without WWI^^		54.13	54.74
Counterfactual Life Expectancy without WWII^^		39.90	39.10
Counterfactual Life eExpectancy^^		56.22	55.97

*Hump is modeled as a accident rate that starts in adolescence, set to happen at (- 0.0175 * calendar year) + 47.4 + 1 based on the estimates provided in de La Rochebrochard (2000) for the onset of menarche among girls and the assumption that adolescence starts one year later for men.

**The estimates in this row correspond to the value of the parameter during the world wars. For example the first column shows that I was about 1.1417 throughout life but decreased to -1.3104 during WWI and decreased to 0.0577 during WWII. The same applies to column (2). In column 2, we allow the shocks in investment to vary across years during WWI. The results show that 1914 was the worst year of the war.

^Our main fit criteria is the sum of squared errors of the survival rate at each age. We also report the fit as the sum of squared errors of the log of q_x (the probability of dying between ages x and $x+1$). We don't target these moments directly–we target the survival curve.

^^Counterfactual Life Expectancy is computed by holding all estimated parameters fixed and setting the war parameters to the parameter I.

~This is computed as sum of squared errors during the war years. A lower number is better.

~~This is computed as (predicted - actual)/actual

To make the fit of the age distribution comparable across columns we use the (normalized) number of deaths as weights.

Table 6: Comparison with alternative mortality models

Cohort			1816					1921		
Model	LMM	G	HP	C	SA	LMM	G	HP	C	SA
Panel A: Women										
Survival curve fit										
RMSE all ages	1.247		0.40	25.78	12.67	1.33		1.08	37.13	6.14
Log of mortality fit										
RMSE (age 45+)	12.05	9.99				3.56	1.34			
RMSE all ages	9.57		9.60	9.61	9.63	3.08		3.08	3.02	3.08
Actual LE	38.28		65.83							
Predicted LE	37.98	-	38.29	17.19	48.09	67.47	-	66.20	69.55	69.37
Panel B Men										
Survival curve fit										
RMSE all ages	1.03		0.49	4.23	5.52	3.28		1.15	2.18	4.90
Log of Mortality fit										
RMSE (age 45+)	14.25	12.10				5.75	3.61			
RMSE all ages	11.44		11.40	11.41	11.40	4.73		4.73	4.73	4.72
Actual LE	35.93		56.14							
Predicted LE	35.94	-	35.95	32.60	39.17	53.65	-	56.65	57.20	58.70
# of parameters	6	2	8	8	6	7	2	8	8	6

note: LMM refers to the model in this paper, G refers to Gompertz (1825), HP refers to Heligman and Pollard (1980), C refers to Carriere (1992) and SA refers to Sharrow and Anderson (2016).

Appendix B: Review of existing models of mortality and contribution of this paper

Aggregate Models in Demography

The primary objective of demographic modeling efforts has been to develop parsimonious parametric models that provide excellent fits to the data and that therefore can be used in various applications such as pricing annuities or projecting the costs social security. A second important objective has been to characterize the differences in the mortality rates across populations and time periods by comparing the underlying parameters of the model for each population. Here we review canonical models as well and the most recent ones.

In a series of seminal papers starting in 1825, Gompertz observed that mortality rates increased exponentially with age in adulthood, a fact that could be used to price annuities (Gompertz was an actuary). Mathematically, the Gompertz function approximates mortality rates (μ_x) in old ages with a log linear function, with one parameter capturing the intercept (α) and the other (β) capturing the slope of (the log) of mortality with age (x):

$$\mu_x = \alpha e^{\beta x}.$$

This model, which came to be known as the Gompertz law, has proved to be an excellent fit for period and cohort data, starting roughly at ages 30-40 and above.[31] The Gompertz law also provides an excellent characterization of the mortality profiles of other species (for a review see Finch et al. (1990)). As a result, subsequent work was devoted to understanding why the Gompertz law arises. The reliability theory from engineer-

[31] Previous work has also shown that the slope of mortality with respect to age is remarkably stable across human populations (Vaupel, 2010) though recent work by Beltrán-Sánchez et al. (2012) shows that the slope of aging varies with early conditions measured by childhood mortality.

ing, which conceptualizes the body as a complex system with many redundant parts, (Gavrilov and Gavrilova, 2001) provided the first mathematical explanation of why the Gompertz law arises.[32] Another important strand of research has investigated the fit of the Gompertz model at very old ages during which mortality appears to plateau instead of continuing its exponential rise.

In a subsequent development Makeham (1860; 1867) noted that some deaths are independent of age, which lead to a modification of the Gompertz law to include a third parameter (γ), capturing what was described as "extrinsic" or age-independent mortality, in contrast to intrinsic or age-dependent mortality which was captured by the Gompertz law. This extended model is often referred to as the Gompertz-Makeham law:

$$\mu_x = \alpha e^{\beta x} + \gamma.$$

The parsimony and empirical success of the Gompertz model also led to many efforts to develop a "unified" theory of mortality that would characterize the evolution of mortality from birth to death (Carnes et al., 1996). The most successful of these efforts is the model by Heligman and Pollard (1980)—henceforth HP.[33] This is an eight-parameter model that describes the probability of dying (q_x) at each age (x) and accounts for three distinct phases of mortality: declining mortality in childhood (3 parameters: A, B and C), the adolescent hump (3 parameters: D, E and F) and exponentially increasing mortality in old ages (2 parameters related to the Gompertz curve: G, the intercept at age 0, and H, the slope).

$$q_x = A^{(x+B)^C} + De^{-E(lnx-lnF)^2} + \frac{GH^x}{1+GH^x}.$$

[32] More recent efforts have tested and refined these theories. See Mitnitski et al. (2015) for a summary. There are several alternative models of aging, for example another set of theories argues that aging is the result of genetic regulated processes (e.g. Moody and Sasser, 2020). A key issue is whether health deteriorates as a function of deficits/failures or as a function of the passage of time (or both).

[33] Siler (1979, 1983) provided a six parameter model from birth to death. However, this model does not fit many populations well as it fails to account for the adolescent accident hump.

A large number of subsequent papers has used this model and demonstrated that it provides an excellent fit for period data from various contexts as Sharrow et al. (2013) describe. This model is popular for several reasons: it is parsimonious, it fits the data well and the parameters have natural interpretations that make it a useful tool in comparing populations.

Other models have been developed since. For example Carriere (1992) introduces a parametric model with slightly better fit for the US male and female 1980 CSO tables. The survival function in Carriere (1992) is a mixture of a Weibull, Inverse-Weibull, and a Gompertz function, and is determined by 8 parameters:

$$s(x) = \psi_1 \exp\left\{-\left(\frac{x}{m_1}\right)^{\frac{m_1}{\sigma_1}}\right\} + \psi_2\left[1 - \exp\left\{-\left(\frac{x}{m_2}\right)^{\frac{m_2}{\sigma_2}}\right\}\right] + (1-\psi_1-\psi_2)\exp\left\{e^{-\frac{m_3}{\sigma_3}} - e^{\frac{x-m_3}{\sigma_3}}\right\}$$

Although the HP model provides an excellent fit to the data it does not break down mortality into different types or causes. A recent paper by Sharrow and Anderson (2016) provides an alternative model that separate mortality into extrinsic and intrinsic lifespans (building on earlier work by Li and Anderson (2013), and extending the Gompertz-Makeham law to all ages). Roughly speaking, extrinsic factors correspond to changes infectious disease and other factors that the environment imposes on the individual; and intrinsic factors are changes in way the body functions and roughly correspond to changes in chronic (non-communicable) diseases. The model has two functions that characterize extrinsic mortality in childhood and mid-life, and one that characterizes intrinsic mortality in old age. This model does characterize the evolution of mortality from birth to death, but the authors fit their model to period not cohort data. Their objective is to separate into causes of decline, not to provide a model that is a better fit to the data than previous ones, or to explain other phenomena.

The HP model is also not well suited to understand how insults early in life affect mortality later in life. Palloni and Beltrán-Sánchez (2017) have a model of Barker frailty,

linking frailty early in life with mortality at various points in the lifetime. It characterizes frailty in three portions of the lifetime, where frailty results in excess mortality early and late in life but not in the middle portion. This paper does not estimate the model, it conducts simulations to understand the effects of increasing frailty on mortality patterns. This model is not estimated with any data so it is difficult to assess how it would compare to other models in terms of fit, including ours.

All demographic models describe aggregate mortality rates as a function of various parameters.

This paper makes main contributions to the existing literature in demography. First, we provide a parsimonious and tractable production function that describes the evolution of a population's health and mortality starting at birth that is suited for tracking the long-term impacts of various insults and investments. To that end, our approach differs in one fundamental aspect from the demographic approach just described. As in the seminal Grossman (1972) model, we model directly how the health stock of each individual evolves, rather than only modeling the mortality or survival rates of the aggregate population.

Like the HP model, our model flexible enough to provide an excellent fit for the mortality profiles of more than 100 cohort we study. But our approach is better suited for studying how various shocks affect the health and mortality of the population overtime — we can easily model inputs into health directly and trace their effects as cohorts age by tracking the evolution of the distribution of health. Relative to the recent models our model has some advantages. Like Sharrow and Anderson (2016) we decompose mortality into two separate causes of death, extrinsic and intrinsic. Like Palloni and Beltrán-Sánchez (2017) we can use our model to study Barker frailty. Our model accomplishes both aims within the same framework.

The second main contribution of this paper is to show that simple modifications of this baseline model explain a wide range of existing demographic phenomena. We demon-

strate this by studying the effects of increasing lifetime resources, and the impact of negative in utero shocks on a population's subsequent average health and mortality. We also study the effects of temporary shocks such as wars or bad weather. To our knowledge there is no other model that both provides an excellent fit to the cohort data and that can also explain the variety of phenomena we study.

Before moving onto the economics models, we also note that our paper builds on the classic demographic work by Vaupel et al. (1979) to introduce heterogeneity in the population from birth onwards.

Models of Individual Mortality in Economics

Economic models of health and mortality were not developed with the aim of fitting aggregate demographic data. Instead, they were developed to understand health expenditures and health behaviors and thus focus on how individuals would maximize their wellbeing (or utility) which depends on health and consumption. In addition to including parameters that govern the evolution of health and longevity, these models also include other "deep" parameters regulating for example the extent to which individuals value health relative to consumption or their discount rates.

The study of health and health behaviors in economics dates back to the seminal model of Grossman (1972). The objective of this model is to derive the demand for medical care (and thus to explain medical care spending) as a function of an individual's characteristics (including education and other traits), their wages and the prices of medical care. The model posits that the demand for medical care is derived from the demand for health, which individuals value itself (it has consumption value) and because health affects productivity in the labor market and thus affects wages. Because health is the ultimate good individuals are after, Grossman models its evolution until an individual dies. Importantly, Grossman's model assumes i) that individuals face a constantly depreciating health, which depreciates as a function of the existing stock, and ii) that they can invest

in (and restore) their health by purchasing market goods and services and investing their own time. In this model factors that affect the cost of these investments (such as wages or prices) modify behavior and ultimately health and mortality.

This model is the starting point for almost all studies in economics that investigate individual health and mortality. Its insights have been cited to explain a wide range of phenomena, including, for example, SES gradients in health. There have also been several attempts to estimate this model using cross sectional and more recently panel data (for a review of early attempts, see Grossman (2004)). However, these attempts have rejected the Grossman model empirically on a number of dimensions. For instance the model predicts that health investments are highest for the healthiest individuals, whereas the data show the opposite is true (for a recent summary of these attempts, see Hartwig and Sturm (2018)).

Over the years the model has faced further criticism. Particularly relevant to our contribution, previous authors have noted that the model is unrealistic in its conception of health. In Grossman (1972)'s model individuals can perfectly restore their health and in principle they could live forever. The model also starts with adults. Thus, a number of models have been developed to address some of these issues. Two recent models address some of the limitations of the Grossman model.

Galama and Van Kippersluis (2019)'s model is designed to understand how socioeconomic status affects health over the life cycle. The original Grossman model allows for differences in education and income/wages to affect the demand for health though limited channels. However empirical work has demonstrated that the SES gradient in health likely operates through many other dimensions (e.g., job related stress, affecting the rate of health deterioration), which Galama and van Kippersluis incorporate. Galama and van Kippersluis calibrate their model and show that its predictions are consistent with observations in the literature.

Dalgaard and Strulik (2014) develop an alternative model where individuals also make

multiple choices regarding consumption, savings and health investments. They use this model to assess if the famous Preston curve, relating GDP to life expectancy, can be understood as resulting from the effects of income on longevity through investments. The key difference in this model is how aging is modeled: based on insights from gerontology, aging is described as the result of cumulative health deficits. The authors calibrate the model and then show that changes in GDP generate predictions that line up with the observed Preston curve. Unlike the Grossman model, this model predicts that unhealthy individuals spend more on health than healthy individuals, and they cannot live forever regardless of how much they invest in health.

Like all the previous economic models, both Galama and Van Kippersluis (2019)'s and Dalgaard and Strulik (2014)'s models start in adulthood. Dalgaard et al. (2019) extend the previously developed health deficit model of Dalgaard and Strulik (2014) to incorporate the childhood period to be able to study the long-term impact of in utero and childhood conditions. During the childhood period individuals grow. They calibrate this model and show that in contrast to the Grossman model, this model predicts that differences in health early in life are amplified during the lifetime of individuals. They do not make predictions about mortality profiles.

Our basic model is more parsimonious than the original Grossman model, or its most recent successors in the economics literature (Dalgaard and Strulik (2014) or Galama and Van Kippersluis (2019)). These models were developed to understand health expenditures and health behaviors and thus focus on how individuals would maximize their wellbeing (or utility) which depends on health and consumption. As a result, these economic models can only be estimated if one has access to incomes/wages, prices, health care utilization and other variables. We use data on mortality alone to calibrate our model. We a focus on a production process only and ignore maximizing behavior, at least initially. In this dimension, our model differs in a number of other dimensions from the original Grossman model. For example, we do not impose a maximum life expectancy, we incor-

porate stochastic shocks, we allow for differences in initial endowments and our aging process does not depend on the level of health.

Our main innovation relative to these more ambitious models is to provide a unified framework for health and mortality at all ages, including childhood. Including this key childhood period allows us to match the pattern of declining mortality among children (up to adolescence). Alternative state-of-the art models, such as Dalgaard and Strulik (2014)'s accumulating health deficits model, or Galama and Van Kippersluis (2019)'s theory of socioeconomic status and mortality, start with adults and thus cannot account for this feature of the data.

Dalgaard et al. (2019) extend Dalgaard and Strulik (2014)'s model to include a childhood period, but they do so by adding a separate health production function for childhood. Instead, our framework is able to describe aging from birth to old ages with the same law of motion, where mortality declines during childhood due to both selection effects and investments. We also demonstrate that the model fits mortality curves for entire cohorts well, which more ambitious economic models have not demonstrated. To our knowledge, there is no other model that has accurately (empirically) predicted the lifetime health and mortality of populations, while providing a law of motion for health at the individual level. By tracking the evolution of health for all individuals in entire population and its mortality consequences, our model provides a framework that bridges the economic and demographic approaches and upon which more complex models that incorporate behaviors can be built and estimated.

It is worth noting that our model's predictions for the effects of in utero shocks do not perfectly align with those of the health deficit model as we note in the text: Dalgaard et al. (2019)'s model of health deficits also predicts that in-utero shocks will result in health gaps that increase with age starting in adulthood. Our model predicts a U-shape pattern of effects rather than a monotonically increasing effect. This U-shape results from our having an early childhood period where investments move the distribution of health up.

Appendix C: Mathematical appendix

The model is defined as follows:

$$\begin{cases} H_a = H_{a-1} - d(a) + I + \varepsilon_t \quad \text{if } D_{a-1} = 0 \\ D_a = \mathbb{I}(H_a \leq \underline{H}, D_{a-1} = 0), \\ D_0 = 0 \end{cases} \tag{1}$$

with $d(a) = \delta \cdot a^\alpha$ $\delta \in (0, \infty)$, $\alpha \in (0, \infty)$, and $I \in \mathbb{R}$. $\underline{H}$ and σ_H^2 are normalized to be 0 and 1, respectively. Let $\hat{H}_a \equiv \mathbb{E}\left[H_a \mid H_a > 0\right]$ denote the average health in the living population with age a and $\sigma_{\hat{H}_a} \equiv Var\left[H_a \mid H_a > 0\right]$ the variance of health among the living.

Proposition 1. ***Everyone dies eventually.***

The cumulative distribution function of our process can be bounded above by a process easier to study. Consider the process $\{H_a^*\}_{a=1}^{\infty}$, defined by $H_0^* = H_0 \sim \mathcal{N}\left(\mu_H, \sigma_H^2\right)$ and the recurrence relation:

$$H_a^* = H_{a-1}^* + I - \delta \cdot a^\alpha + \varepsilon_a \ , \ \varepsilon_a \sim \mathcal{N}\left(0, \sigma_\varepsilon^2\right) \tag{2}$$

The process is similar to the one in our model except that there is no truncation. It is easy to tell that $0 \leq P\left(H_a > z\right) \leq P\left(H_a^* > z\right)$ for any $z > 0$. Now for any $a \geq 0$, H_t^* is normally distributed with mean

$$\mu_{H_a^*} = \mu_H + I \cdot a - \delta \sum_{k=1}^{a} k^\alpha \tag{3}$$

and standard deviation

$$\sigma_{H_a^*} = \sqrt{\sigma_H^2 + a \cdot \sigma_\varepsilon^2} \tag{4}$$

Hence, $P\left(H_a^* > z\right) = 1 - \Phi(\frac{z - \mu_{H_a^*}}{\sigma_{H_a^*}})$, where Φ is the CDF of the standard normal distribution. As $a \to \infty$, we have $\mu_{H_a^*} \sim I \cdot a - \delta \cdot \frac{a^{\alpha+1}}{\alpha+1}$ and $\sigma_{H_a^*} \sim \sqrt{a} \cdot \sigma_\varepsilon$. Therefore if $\alpha > 0$, $\frac{\mu_{H_a^*}}{\sigma_{H_a^*}} \to -\infty$ as $a \to \infty$.

Remark: Extended model with Accident shocks Proposition 1, 2 and 3 hold for the extended model with accident shocks drawn independently from the health status. Because accident shocks are drawn independently from the health status, they leave the *cdf* of health unchanged and therefore the proofs are unaffected.

Appendix D: Notes on the empirical methods

1. Data

Territory changes. The table below describes the details of the changes in territory that took place in France since 1816.

Year	Territorial Changes
1861	Annexation of Savoie and Haute-Savoie, and of *Comte* de Nice
1869	Franco-Prussian war: loss of Alsace-Lorraine
1914	WWI: East of France, is occupied by German military.
1919	At the end of WWI, Alsace-Lorraine is re-integrated to French territory
1939	WW2: Loss of Alsace-Lorraine
1943	WW2: Loss of Corsica
1945	Current territory: Alsace-Lorraine and Corsica re-integrated to French territory

These changes in territory results in large changes in the population and death counts. This is illustrated below for population. It is unclear how to compute mortality in the year of the change. We compute it by using a weighted average of the population at the beginning and end of the year.

Migration. In the HMD, cohort population counts are available. However, because of migrations, these counts cannot be used to derive a survival curve for a cohort. Because of net positive immigration occurring in France, the number of individuals in a given cohort can even increase from one year to the next. This is especially true at the end of the Algerian Independence War. (e.g. the size of the female cohort born in 1910 increases from $300,369$ to $303,273$ between 1962 and 1963, despite a reported mortality rate of 0.5162. The unit of analysis in our model of mortality is a country cohort, hence abstracts from migration. In our model the mortality rates coincide exactly with the slope of the survival curve. This is not true in the HMD. The population of the cohort melts natives and immigrants of the same age.

2. Computing the death rates, survival rates and life expectancy

Death rates. When taking our model to the data we target the most direct counterpart of our modeled cohort "mortality rate", which is computed as the number of individuals who died during a year, divided by the number of individuals alive at the beginning of the day. Technically, we compute annual probabilities of dying at a given age instead of rates. We make no adjustments for the fact that the deaths in the first year do not correspond to individuals born that year.

In typical life tables this number corresponds to what demographer call q_t, the probability of dying in a given year, and is conceptually distinct to the mortality rate, denoted by m_t. The main difference lies in adjusting the denominator — the size of the population. As more individuals die during the year the population needs to be adjusted to estimate the size of the remaining population exposed to the risk of death. Because our baseline model does not take this adjustment into account, we compute a direct counterpart of our theoretical object. Therefore, we compute the raw death rate in year t for a given cohort , q_t , as follows:

$$q_t = \frac{D_t}{N_t}$$

where D_t is the death count for year t from the HMD cohort table and N_t is the population on January 1st of year t. The HMD makes adjustments to compute a probability that is corrected for the fact that the data do not tract the same individuals over time, so the probability of dying is not correctly computed for a given cohort. The q we estimate with the raw counts is very similar to what is reported by the HMD except for the first year of life and the last years of life as shown in Appendix Figure 9. This results in our underestimating life expectancy somewhat.

Survival curves. We compute the survival curve recursively as follows. After initial-

izing $S_0 = 100$, we iteratively compute:

$$S_t = S_{t-1} \times (1 - q_{t-1})$$

Life expectancy. Life Expectancy (LE) is an important statistics for the health profile of a given cohort. We compute LE as a way of comparing our model to the data in a parsimonious way. While we try to provide informative estimates of cohort life expectancy, we do not claim that their accuracy is comparable to demographic studies. Nevertheless, as we treat the series generated by our model in exactly the same manner as the data series, we obtain pairs of LE that are readily comparable.

3. Estimation routine

We compute our estimates using Matlab's canned *fminsearch* routine, a downhill simplex method, and Powell (1964)'s conjugate direction method. We first estimate the model using *fminsearch* until the objective function changes by less than 10^{-3}. The objective function is the sum of squared errors between the model's survival's curve and the one from the data. We then use these estimates as starting values for Powell's routine. Once Powell's routine converges, we use the estimated values from this procedure and implement *fminsearch* again until it converges. The total estimations on the UCLA computing cluster takes several hours. We experimented with different initial values for the parameters. The reported estimates correspond to the lowest final function value.

4. Bootstrapping standard errors

Estimates from sample data come with standard errors. However, the mortality rates in the HMD are computed from birth certificates of the total population, not a sample of it. A typical cohort in our study counts $400,000$ individuals. As a result, the standard errors are negligible and all of the parameter uncertainty comes from model mispecification

and data inaccuracy rather than sampling variation. We therefore do not report standard errors for the French cohorts.

In contrast, we do compute the standard errors for the chimpanzee estimates as the data in that case consist of samples of one or two hundreds of individuals. One way of bootstrapping the standard errors, given a series of mortality rates for a cohort, is to view each sample of size N as a sequence of Bernoulli trials with varying success rates. Alternatively, one can view the survival curve of a population of size N as an $N \times 1$ vector of age at death. One can produce bootstrap estimates by drawing with replacement M subsamples of size N and compute the empirical survival curve.

5. Estimation of Wars/pandemics in time series

We estimate the complete times series for females only. We model WWI and WWII as lowering the level of I during the event, which is set to start in 1918 and last one year in the case of the flu pandemic for women–this choice is motivated by the data which shows that WWI did not result in an increase in mortality for them, but instead mortality increased dramatically as a result of the Flu (see Appendix Figure 10). For men we lower I from 1914 to 1919 (see Appendix Table 5). For WWII we lower I from 1939 to 1945.

6. Estimation of alternative mortality models

We estimate four alternative models of mortality. We use the R package "MortalityLaws" version 1.9.3 (developed by Pascariu and Canudas-Romo, 2022) to estimate the Gompertz (1871), Heligman and Pollard (1980) and Carriere (1992) models, and the package "vitality" version 1.3 (developed by Passolt et al., 2018) to estimate the Sharrow and Anderson (2016) model.[34] We estimate the Gompertz model for age 45 onwards only. All models are

[34]While usually estimated on period data for practical reasons, several of these models have a natural "cohort" interpretation, e.g. the vitality process in Sharrow and Anderson (2016) alludes to physiological processes occurring at the individual level.

estimated only up to age 100. We use the predicted values from each model to compute the RMSE, as $RMSE = \sqrt{\frac{1}{100}\sum_{a=0}^{99}(y_a - \hat{y_a})^2}$

Appendix E: Implications for optimal investments

Optimization in a stationary environment

So far we have considered a population that receives constant investments in its health, uniformly over the lifetime. But is that behavior a reasonable approximation if resources are optimally allocated over the lifetime? To answer this question, this section relaxes the simplifying assumption of constant investment, and estimates the optimal investment profile that a social planner concerned with maximizing the life-expectancy of a population would choose. Remarkably, while this optimal investment profile indeed deviates from the constant investment rule studied in the previous sections, it would result in very similar patterns of mortality. In other words, the optimal investment sequence does not fundamentally change the age-profile of mortality rates. We then evaluate the life expectancy gains resulting from optimization.

First, we develop notation to describe the problem that a benevolent social planner would face. We solve this problem under two key assumptions. The first key assumption is that the planner has a fixed budget but has the ability to borrow and save costlessly — in other words, the planner knows exactly what the total lifetime resources are for a given cohort and can redistribute these resources across the lifetime at no cost.[35] The second assumption we make is that the planner wishes to maximize life expectancy.

The survival function tracks the probability of surviving over time. It is naturally expressed as a function of the cdf of health in the population. The probability of surviving until the end of period a is $S_a = 1 - F_a(0)$. Life expectancy at birth for a given cohort is conveniently related to the survival function

$$LE = \sum_{a=1}^{\infty} S_a$$

[35] This is a standard set of assumptions in this type of models, for example see Murphy and Topel (2006).

Several observations are in order. First, in practice, this is a finite sum. Second, this is the cohort's life expectancy, not the "period" life expectancy which is usually reported. The social planner now chooses an investment path $\mathcal{I} = \{I_a\}_{a\in\mathbb{N}}$ that is age-dependent, instead of keeping the investment level I constant over the lifetime. The planner can move resources over time periods costlessly, as if a perfect annuity were available, and faces a given lifetime budget, B. Then the optimization problem takes the form

$$\begin{aligned} \max_{\mathcal{I}} LE(\mathcal{I}) &= \max_{\{I_a\}} \sum_{a=1}^{\infty} S_a(\mathcal{I}) \\ s.t. \quad & \sum_{a=1}^{\infty} I_a \cdot S_a(\mathcal{I}) \leq B \end{aligned}$$

The social planner chooses an optimal path such that the marginal effect of increasing investment at a given age is equalized across all ages. The first order conditions are given by

$$\sum_{s=a}^{\infty} \frac{\partial S_s(\mathcal{I})}{\partial I_a} - \lambda \left[S_a(\mathcal{I}) + \sum_{s\geq a}^{\infty} I_s \frac{\partial S_s(\mathcal{I})}{\partial I_a} \right] = 0 \ , \forall a > 0$$

where λ is the Lagrange multiplier and therefore $\frac{1}{\lambda}$ represents the shadow cost for the social planner, starting from the optimal path, of an additional year of life expectancy. Both terms in the bracket are positive, illustrating the key dynamic tradeoff in investment with a fixed budget. An additional investment at one age increases the number of survivors at all subsequent ages, exerting greater pressure on the budget at all subsequent periods. Intuitively, this channel gets weaker and weaker at older ages because mortality rates are high at old ages even with investments. While we were unable to formally makes this point analytically, we show numerically that this intuition is valid in the range of parameters estimated from the data.

Timing of optimal investments, polynomials

To estimate the optimal investment, we follow a lower-dimensional sieves estimation method.[36] We start by approximating the investment profile over age with a first order function of age (adding 2 parameters) and then with a second order polynomial (3 more parameters). We impose the constraint that the total spending per cohort is the same as the budget resulting from our estimated constant lifetime investment i.e. $B = \sum_{a=1}^{100} \hat{I} \cdot S_a(\mathcal{I})$. Given budget B we run a grid search to find the quadratic investment profile that maximizes the life expectancy of the cohort.

The results of this exercise are displayed in Appendix Figure 21. Relative to the case with a constant function, an optimal linear investment function redistributes more resources to the young. If we allow a quadratic term then we find that a U-shape investment profile is optimal to maximize the average life-expectancy in the population (panel a). Our original model sets I to be constant in levels. But in percentage terms, relative to the baseline level of health at a given age, I was already U-shaped in the basic model. What we find then is that the optimal investment is even more U-shaped — it transfers additional resources to the young and the old, away from the middle-aged individuals.

These results show that optimal health investments are largest when health is at its lowest — that is, at very young and very old ages. Interestingly, health care expenditures by age in most countries actually follow this age-profile (Alemayehu and Warner, 2004). These findings are also consistent with empirical findings which show that health and the demand for medical services are negatively correlated (Wagstaff, 1986) and that medical expenditures rise sharply with age (e.g. De Nardi et al. 2010).[37]

[36] A fully nonparametric approach for the optimal investment profile over the lifetime would require optimizing over a hundred or so parameters (one for each age) for each cohort. In the absence of a closed-form solution, this is impractical. It is also not feasible since we have 100 data points: if we allow for a unique investment level at every age we are under-identified (we would have 100 data points and at least 106 parameters to estimate).

[37] These results are in contrast with the predictions of the Grossman model which predicts that investments would decline with age as individuals near death. See Wagstaff (1986) for an early discussion, or Strulik (2015) for a more recent discussion of this issue.

Panel b shows the mortality curves before and after optimization — they have the same basic shape we have observed. The resulting survival curves are flatter in adulthood and steeper in old ages, suggesting the rectangularization of survival might be in part associated with the emergence of optimal investments. Optimizing investment results in a gain of about 3 years of life expectancy in the specific case we show in Appendix Figure 21, based on the estimated parameters for French women born in 1816.

Optimization when budgets depend on health. We have solved the optimization problem under the assumption that stock of available resources is not influenced by the health of the population. But if food and other resources are produced rather than taken from the environment, health is likely to impact resources by affecting the work capacity of the population. Indeed, nutrition levels and disease rates have been shown to affect productivity and wages (Thomas et al., 2004). They also affect inputs into wages such as cognition and education (Field et al., 2009). Many empirical studies report a correlation between income and health (Cutler et al., 2012, Chetty et al., 2016) as noted above. While our baseline model embeds the effect of resources on health, a causal link going in the other direction is also likely at play: people who get sick or are hospitalized suffer a subsequent drop in income (Smith, 1999, Dobkin et al., 2018). With panel data on wages, it would be possible to improve on our estimates to account for these effects.

Overlapping generations. Another natural extension would be to embed our model in an overlapping generations setting to reflect the fact that most social insurance programs, including health care insurance, involve transfers across cohorts at a given point in time, rather than within-cohort transfers over time (as we have considered here for simplicity). An overlapping generation model could also be used to link the health of the parents with that of their children, a mechanism that has found some support in the empirical literature.